Long-term observational constraints of organic aerosol dependence on inorganic species in the southeast US

Yiqi Zheng[1,2,*], Joel A. Thornton[3], Nga Lee Ng[4,5,6], Hansen Cao[7], Daven K. Henze[7], Erin E. McDuffie[8,9], Weiwei Hu[10,11], Jose L. Jimenez[11], Eloise A. Marais[12,13], Eric Edgerton[14], Jingqiu Mao[1,2,*]

[1]Geophysical Institute, University of Alaska Fairbanks, Fairbanks, AK, USA
[2]Department of Chemistry and Biochemistry, University of Alaska Fairbanks, Fairbanks, AK, USA
[3]Department of Atmospheric Sciences, University of Washington, Seattle, WA, USA
[4]School of Chemical and Biomolecular Engineering, Georgia Institute of Technology, Atlanta, GA, USA
[5]School of Earth and Atmospheric Sciences, Georgia Institute of Technology, Atlanta, GA, USA
[6]School of Civil and Environmental Engineering, Georgia Institute of Technology, Atlanta, GA, USA
[7]Department of Mechanical Engineering, University of Colorado Boulder, Boulder, CO, USA
[8]Department of Physics and Atmospheric Science, Dalhousie University, Halifax, Nova Scotia, Canada
[9]Department of Energy, Environmental & Chemical Engineering, Washington University in St. Louis, St Louis, MO, USA
[10]State Key Laboratory of Organic Geochemistry, Guangzhou Institute of Geochemistry, Chinese Academy of Science (CAS), Guangzhou, China
[11]Department of Chemistry and CIRES, University of Colorado Boulder, Boulder, CO, USA
[12]School of Physics and Astronomy, University of Leicester, Leicester, LE1 7RH, UK
[13]Now at Department of Geography, University College London, London, UK
[14]Atmospheric Research & Analysis, Inc., Cary, NC, USA

[*]Correspondence to: Yiqi Zheng (yzheng4@alaska.edu) and Jingqiu Mao (jmao2@alaska.edu)

Keywords: Secondary organic aerosol; IEPOX; isoprene; coating; aerosol acidity.

Abstract

Organic aerosol (OA), with a large biogenic fraction in summertime southeast US, adversely impacts on air quality and human health. Stringent air quality controls have recently reduced anthropogenic pollutants including sulfate, whose impact on OA remains unclear. Three filter measurement networks provide long-term constraints on the sensitivity of OA to changes in inorganic species, including sulfate and ammonia. The 2000-2013 summertime OA decreases by 1.7~1.9%/year with little month-to-month variability, while sulfate declines rapidly with significant monthly difference in early 2000s. In contrast, modeled OA from a chemical-transport model (GEOS-Chem) decreases by 4.9%/year with much larger monthly variability, largely due to the predominant role of acid-catalyzed reactive uptake of epoxydiols (IEPOX) onto sulfate. The overestimated modeled OA dependence on sulfate can be improved by implementing a coating effect and assuming constant aerosol acidity, suggesting the needs to revisit IEPOX reactive uptake in current models. Our work highlights the importance of secondary OA formation pathways that are weakly dependent on inorganic aerosol in a region that is heavily influenced by both biogenic and anthropogenic emissions.

1. Introduction

Organic aerosol (OA) accounts for a large fraction of ambient fine particulate matter mass, which strongly affects air quality, regional climate, and human welfare (Jimenez et al., 2009). Since the implementation of the Clean Air Act Amendments of 1990, there has been a significant decline in ambient aerosol in the United States, mostly due to reductions in inorganic aerosol mass following changes in emissions of sulfur dioxide (SO_2), nitrogen oxides (NO_x =NO+ NO_2), as well as reductions in black carbon (EPA, 2011), leaving OA as the major component of fine particulate matter (50~70%) over the southeast US, especially in summer (Attwood et al., 2014; Kim et al., 2015). OA can be directly emitted by combustion processes (primary organic aerosol, POA) or secondarily formed (SOA) from the atmospheric oxidation of biogenic volatile organic compounds (BVOCs), mainly isoprene and monoterpenes, and also precursors from anthropogenic sources and biomass burning (Hayes et al., 2015; Hodshire et al., 2019). OA has also been declining across much of the US over the past few decades, primarily due to decreased anthropogenic emissions from vehicle and residential fuel-burning, except for the southeast US (Ridley et al., 2018). The southeast US is one of the largest BVOC emission hotspots in the world (Guenther et al., 2006), and at the same time is heavily populated with large anthropogenic emissions of pollutants. Biogenic SOA (formed from atmospheric oxidation of BVOCs) may account for 60-100% of OA in summertime southeast US (Kim et al., 2015; Xu et al., 2015b). To what extent biogenic SOA could be mediated through emission control strategies remains an open question (Carlton et al., 2010; Mao et al., 2018).

The oxidation of BVOCs produces hundreds of intermediate products. Some products have low volatility that can partition onto the condensed phase, while some gas-phase products can react in

41 the aqueous phase to form SOA. SOA formed from uptake of isoprene epoxydiols (IEPOX-
42 SOA) (Paulot et al., 2009) appears to be the major confirmed aqueous SOA product globally,
43 being important in all high isoprene and lower NO regions (Hu et al., 2015), along with glyoxal
44 formed from isoprene and aromatics (Fu et al., 2008). Formation of SOA in clouds was
45 investigated in the southeast US and found to be not statistically significant (Wagner et al.,
46 2015). These pathways have been implemented into 3-dimensional global atmospheric chemistry
47 and climate models using two different approaches. First, to simulate the partitioning of organic
48 vapors, the BVOC oxidation products can be grouped based on their volatility (Volatility Basis
49 Set, VBS), and the product yields and vapor pressures are parameterized for each surrogate
50 precursor (Donahue et al., 2006; Pankow, 1994). Such empirical VBS schemes are usually
51 derived using dry laboratory chamber experiments (with relative humidity RH<10%) and do not
52 explicitly depend on aerosol water, RH, or inorganic aerosol mass or composition. Therefore,
53 here we refer to the SOA formed through partitioning calculated by VBS as dry SOA. Second, a
54 more explicit representation of aqueous SOA formation from isoprene products has been used
55 recently, which incorporates dependence on inorganic aerosol volume and aerosol acidity
56 (Budisulistiorini et al., 2017; Ervens et al., 2011; Fu et al., 2008; Marais et al., 2016; Pye et al.,
57 2013). The relative contribution of dry versus aqueous SOA to total OA mass in the atmosphere
58 is uncertain and has limited observational constraints.
59
60 Long-term field measurements show a decreasing trend of OA in the southeast US (Attwood et
61 al., 2014; Hidy et al., 2014; Kim et al., 2015), which is likely linked to reductions in
62 anthropogenic POA and SOA (Blanchard et al., 2016; Ridley et al., 2018), sulfate (Blanchard et
63 al., 2016; Malm et al., 2017; Marais et al., 2017; Xu et al., 2015b, 2016) and NO_x (Carlton et al.,

2010; Pye et al., 2010, 2019; Xu et al., 2015b). The influence of sulfate on OA is thought to be mainly due to its influence on the uptake of isoprene gas-phase oxidation products, which are often small molecules that cannot directly condense due to high vapor pressure, but may undergo aqueous-phase reactive uptake onto wet sulfate particles to form aqueous SOA, as suggested by extensive laboratory and field studies (Budisulistiorini et al., 2015; Hu et al., 2015; Li et al., 2016; Liggio et al., 2005; McNeill et al., 2012; Riedel et al., 2016; Shrivastava et al., 2017; Surratt et al., 2010; Tan et al., 2012; Xu et al., 2016, 2015b). NO_x plays a complex role in regulating oxidation capacity, different oxidation pathways and aerosol water content through aerosol nitrate (Kiendler-Scharr et al., 2016; Kroll et al., 2005, 2006; Li et al., 2018; Ng et al., 2017; Presto et al., 2005; Shrivastava et al., 2019; Zheng et al., 2015; Ziemann and Atkinson, 2012). Prior 3-D modeling studies with different SOA mechanisms provide different explanations for the long-term OA trend observed in the southeast US. For example, the dry SOA calculated by VBS framework with NO_x-dependent yields implies a small decrease in OA following the reductions of NO_x (Pye et al., 2013; Zheng et al., 2015), but has little dependence on changes in inorganic aerosol mass such as sulfate. On the other hand, models using aqueous SOA formation from isoprene attributed the decreasing OA from 1991 to 2013 to reductions in sulfate (Marais et al., 2017) but showed greater interannual variability than was observed. The driving mechanism for the OA trend in the southeast US remains to be elucidated.

Here we use observations from three surface filter-based networks (IMPROVE, SEARCH, CSN), combined with a 3-dimensional chemical transport model GEOS-Chem v12.1.0, to examine the long-term trend and more importantly, the month-to-month variability of OA in the

86 southeast US during 2000-2013. The results provide new observational constraints on the drivers
87 of OA variability and the SOA formation mechanisms in the southeast US.
88

89 # 2. Methods

90 **2.1 Observational datasets.**

91 We use surface filter-based measurement of fine particulate matter mass and composition
92 (including organic carbon, OC) in 2000-2013 from three networks: the Interagency Monitoring
93 of Protected Visual Environments (IMPROVE) (Solomon et al., 2014), the SouthEastern Aerosol
94 Research and Characterization (SEARCH) (Edgerton et al., 2005), and the Environmental
95 Protection Agency's $PM_{2.5}$ National Chemical Speciation Network (CSN) (Solomon et al.,
96 2014). We select 21 IMPROVE sites, 3 SEARCH rural sites and 36 CSN sites within the
97 southeast US region [29°~37°N, 74°~96°W] (Figure S1). The SEARCH sites are organized in
98 rural/urban pairs (Edgerton et al., 2005) and only the data from the rural sites are used here to
99 represent background conditions. IMPROVE sites are mostly rural (Solomon et al., 2014). The
100 OC measurement in the CSN network in 2004-2009 gradually shifted to a different protocol and
101 analytical technique than the early 2000s, which led to the discontinuity in long-term trend
102 (Figure S2), therefore we only use CSN data to examine the monthly variability of OA, and
103 focus on IMPROVE and SEARCH for all analysis. The 3-day OC measurement from IMPROVE
104 and daily OC from SEARCH and CSN are averaged to monthly values. A factor of 2.1 is used to
105 convert measured organic carbon (OC) to organic aerosol mass, as suggested by the southeast
106 US field measurements (Pye et al., 2017; Schroder et al., 2018).
107

We use OA measurements by Aerosol Mass Spectrometer (AMS) from the Southern Oxidant and Aerosol Studies campaign (SOAS) at the Centerville, AL Site in 06/01/2013-07/15/2013 (SOAS2013). The OA measurements and derived IEPOX-SOA factor calculated by Positive Matrix Factorization (PMF) analysis (Hu et al., 2015; Xu et al., 2015a, 2018) are from two independent groups: one group from Georgia Institute of Technology led by Prof. Nag Lee Ng, the other from University of Colorado Boulder led by Prof. Jose L. Jimenez, denoted as Obs_GT and Obs_CU, respectively.

2.2 Modeling framework

2.2.1 GEOS-Chem

In this study we use the 3-dimensional global chemical transport model GEOS-Chem version 12.1.1 (DOI: 10.5281/zenodo.2249246, https://github.com/geoschem/) with detailed O_3-NO_x-HO_x-CO-VOC-aerosol tropospheric chemistry (Bey et al., 2001; Mao et al., 2013). Isoprene chemistry is described in (Fisher et al., 2016; Travis et al., 2016). GEOS-Chem is driven by offline meteorology 1999-2013 from the NASA Modern-Era Retrospective analysis for Research and Applications, version 2 (MERRA-2 https://gmao.gsfc.nasa.gov/reanalysis/MERRA-2/). The global anthropogenic (including agricultural) emissions are from the Community Emissions Data System (CEDS) inventory, with the US region replaced by the EPA's National Emission Inventory for 2011 (NEI11v1). The monthly mean anthropogenic emissions of CO, SO_2, NO_x, NH_3, VOCs, OC and black carbon are scaled to the year 2011 using the ratio of EPA's national annual emission totals from 2000 to 2013 (Travis et al., 2016). Biomass burning emissions are from Global Fire Emissions Database version 4 (GFED4) (Randerson et al., 2015). Biogenic emissions of isoprene and terpenes are online calculated by the Model of Emissions of Gases and

Aerosols from Nature (MEGAN2.1) (Guenther et al., 2012) that is also driven by MERRA-2 meteorology.

For organic aerosol, we employ the complexSOA scheme for SOA modeling for all simulations in this study (Marais et al., 2016; Pai et al., 2020; Pye et al., 2010). POA are regarded as nonvolatile. This SOA modeling includes a 4-product Volatility-Basis-Set (VBS) for SOA formation from reversible condensation of oxidation products of biogenic terpenes (including monoterpenes and sesquiterpenes), and anthropogenic VOCs, referred to as terpene-SOA and anthropogenic SOA, respectively. The SOA calculated through VBS parameterization is fitted based on dry chamber (RH<10%) results independent of inorganic aerosol, aerosol water and RH (Pye et al., 2010). The complexSOA scheme also includes aqueous SOA formed from reactive uptake of isoprene oxidation products, including IEPOX, glyoxal, C_4 epoxides, methylglyoxal, non-IEPOX product of the ISOPOOH oxidation and hydroxynitrates from NO_3-initiated oxidation (Marais et al., 2016). GEOS-Chem v12.1.1 considers sulfate, nitrate, and ammonium from all sectors, and fine-mode Na^+, Ca^{2+}, Mg^{2+}, Cl^- from anthropogenic and sea salt sources, and employs the ISORROPIA II thermodynamic model (Fountoukis and Nenes, 2007; Pye et al., 2009; Song et al., 2018) to calculate aerosol water content and aerosol acidity (Pye et al., 2020).

We run the default GEOS-Chem model at 4°×5° latitude by longitude continuously from 10/01/1999 to 12/31/2013. For each year, the restart file at 05/01 from the continuous 4°×5° simulation has been regridded to 2°×2.5° and is used to initiate 2°×2.5° simulations from 05/01 to 08/31 each year. The May results are discarded as spin-up and the results of June, July and August are used for analysis.

The default modeled OA shows a stronger decreasing trend from 2000 to 2013, and a large month-to-month variability in early 2000s, different from the observations (more details in Figure 1, 2A and Section 3.1). To address this model-observation discrepancy, we do four sets of 2°×2.5° simulations: Default (using default complexSOA scheme); CT (with coating effect for IEPOX reactive uptake); CT_newNH_3 (with coating effect and US NH_3 emissions replaced by satellite-derived NH_3 inventory); CT_H01 (with coating effect and fixing aerosol acidity a_{H+} at 0.1 mol/L when calculating IEPOX reactive uptake). The sensitivity simulations are further explained in Section 2.2.2-2.2.3 and Section 3.3.

2.2.2 Coating

The default IEPOX-SOA mechanism in GEOS-Chem uses aerosol-phase reaction rates from laboratory chamber studies with pure acidic inorganic particles (Gaston et al., 2014; Riedel et al., 2015), and a representative effective Henry's law constant obtained by matching the model to the observations from the SOAS2013 campaign (Marais et al., 2016), to estimate the reactive uptake coefficient γ_{IEPOX}. In the default scheme, γ_{IEPOX} is calculated as follows:

$$\frac{1}{\gamma_{IEPOX}} = \frac{R_p \omega}{4D_g} + \frac{1}{\alpha} + \frac{1}{\Gamma_{aq}} \quad (170)$$

$$\Gamma_{aq} = \frac{4VRTH_{aq}k_{aq}}{S_a \omega} \quad (171)$$

Where R_p is the particle radius of the inorganic sulfate-nitrate-ammonium particle (cm), ω is the mean molecular speed (cm/s), D_g is the gas-phase diffusion coefficient (0.1 cm^2/s), α is the mass accommodation coefficient (α=0.1), S_a is the total (wet) particle surface area (cm^2/cm^3), V is the total (wet) particle volume (cm^3/cm^3), R is the ideal gas constant (L atm/mol/K), T is temperature

(K), H_{aq} is the Henry's law coefficient (1.7×10^7 M/atm), and k_{aq} is the first-order reaction rate constant (s^{-1}):

$$k_{aq} = k_{H^+}[H^+] + k_{nuc}[nuc]a_{H^+} + k_{ga}[ga]$$

where k_{H^+} (=0.036 $M^{-1}s^{-1}$), k_{nuc} (=2×10^{-4} $M^{-1}s^{-1}$) and k_{ga} (=7.3×10^{-4} $M^{-1}s^{-1}$) are the reaction rates due to acid-catalyzed ring-opening, presence of nucleophiles (including nitrate and sulfate) and presence of bisulfate acids, respectively (Gaston et al., 2014; Marais et al., 2016).

In the real atmosphere, inorganic aerosol is generally internally mixed with other organics. The presence of an organic coating may alter the aerosol properties and suppress the uptake of IEPOX onto acidified sulfate aerosol (Anttila et al., 2006; Gaston et al., 2014). We implement a linear coating effect for the IEPOX-SOA formation. The coating effect is fitted using laboratory-derived values of γ_{IEPOX} on particles containing both ammonium bisulfate and ethylene glycol under RH=50% conditions (Gaston et al., 2014). In the coating scheme, γ'_{IEPOX} is calculated as above with R_p, V and S_a updated considering OA coated outside the inorganic core. Then, the fitted function is applied to modify γ'_{IEPOX}:

$$\gamma_{IEPOX\_modified} = \gamma'_{IEPOX} \times (1 - 1.3 \times \chi_{org})$$

where χ_{org} is the mass fraction of OA in the mixed particle including both the inorganic aerosol and OA. When χ_{org}>0.7, the IEPOX uptake will be terminated, i.e. $\gamma_{IEPOX\_modified} = 0$. In the real atmosphere when inorganic cores are coated with more viscous SOA (Zhang et al., 2018b), coating effect may be stronger because ethylene glycol is a low viscosity material. However, this simplified linear function does not consider the decreased viscosity and reduced coating effect at higher RH conditions (which is common in summertime southeast US) (Gaston et al., 2014; Zhang et al., 2018b), and prevents further IEPOX uptake when the mass fraction of OA (χ_{org}) is

larger than 0.7, therefore this linear function may mimic a strong coating effect even though ethylene glycol is less viscous than real atmospheric SOA. The uncertainties need to be addressed in further studies with a more realistic coating parameterization (Li et al., 2020; Schmedding et al., 2019; Zhang et al., 2019b). We assume all OA is coated outside the inorganic aerosol core when calculating the IEPOX reactive uptake. The default GEOS-Chem with no organic coating calculates surface area of inorganic aerosol (Jo et al., 2019). By adding the coating effect, the increased particle radius R_p and surface area S_a of the mixed particle will partially offset (but does not outweigh) the impact of reduced reaction probability $\gamma_{IEPOX\_modified}$.

2.2.3 Satellite-derived NH_3 emissions

We use the Cross-track Infrared Sounder (CrIS) satellite-derived NH_3 emissions (Cao et al., 2020) in a sensitivity test in this study. The top-down monthly NH_3 emissions over the contiguous US at 0.25° × 0.3125° latitude by longitude are derived from CrIS v1.5 measurements of NH_3 profiles (Shephard and Cady-Pereira, 2015) for the year 2014 through a 4D-Var approach using GEOS-Chem and its adjoint model (Henze et al., 2007). The CrIS-derived emissions are then regridded to 0.1°×0.1° to replace the default NEI11 emissions for the year 2011 and applied the same annual scaling factors for 2000-2013. The default NEI11 and CrIS-derived NH_3 emissions averaged over 2000-2013 are compared in Figure S3. There is no significant trend of NH_3 emissions from 2000 to 2013 (Figure S4), consistent with other studies suggesting nearly constant NH_3 emissions from 2001 to 2014 (Butler et al., 2016). The CrIS-derived emissions used the HTAPv2 emissions inventory as the prior emissions, which is based on the 2008 NEI emissions over the US (Janssens-Maenhout et al., 2015). The CrIS-derived NH_3

emissions have been validated against surface observations of NH_3 concentration from the Ammonia Monitoring Network (AMoN) and wet deposition measurements from the National Atmospheric Deposition Program (NADP). More details can be found in Cao et al. (2020). Using the top-down emissions in GEOS-Chem increases the correlation coefficient (r) between modeled monthly mean NH_3 concentration and surface observations from 0.74 to 0.93 and reduces the normalized mean bias of domain-averaged annual mean simulated NH_3 by a factor of 1.9. The seasonal cycle of simulated wet NH_4^+ deposition is also improved (r increased from 0.70 to 0.86), but the normalized mean bias of domain-averaged annual simulated wet NH_4^+ increases from 0.34 to 0.96 due to overly strong wet scavenging in the model. The latter issue was ultimately resolved in Cao et al. (2020) and the final top-down emissions reported therein differ from those reported here; nevertheless, the emissions estimates used here provide a valuable basis for conducting a sensitivity experiment.

2.3 Multivariate linear regression analysis

In this study we did a multivariate regression analysis of modeled monthly IEPOX-SOA (μg/m^3) against modeled sulfate aerosol (μg/m^3), aerosol acidity a_{H+} (mol/L) and isoprene emission ($ISOP_{emis}$ mg/m^2/hr):

$$IEPOX\text{-}SOA = \beta_1 \times sulfate + \beta_2 \times a_{H^+} + \beta_3 \times ISOP_{emis} + b$$

Mean values have been subtracted from all variables, which are then divided by standard deviations. β_1, β_2 and β_3 are standardized partial regression coefficients associated with sulfate aerosol, a_{H+} and isoprene emission, and can be directly compared to evaluate the relative importance of the three variables. We apply the regression analysis using monthly data within

different time frames (2000-2013, 2000-2004, 2005-2008 and 2009-2013 as in Table S1) to determine the evolving importance of variables.

3. Results

3.1 Long-term trend and month-to-month variability (MMV) of OA

In the southeast US, observations from the IMPROVE and SEARCH network both show a reduction in summertime surface OA concentration from 2000 to 2013 (Figure 1). Observational results are averaged using 21 IMPROVE sites and 3 SEARCH sites within the southeast US. OA concentration averaged over June-July-August (JJA) 2000-2013 is 4.2 $\mu g/m^3$ from the IMPROVE sites, and 5.7 $\mu g/m^3$ from SEARCH sites. A similar ~30% summertime low bias on the IMPROVE sites was documented by Kim et al. (2015) compared to the SEARCH sites, which is thought to be due to evaporation of OA from the filters after collection, as the IMPROVE filters stay several days on site after sampling and are shipped without refrigeration, while the SEARCH filters are analyzed in-situ. Despite different magnitudes, OA from the two networks demonstrate similar trends and interannual variability. The 2000-2013 trend of JJA OA mass is -1.7%/year for IMPROVE and -1.9%/year for SEARCH. Compared to the slow decrease in OA, a faster declining trend is found for sulfate from IMPROVE (-6.9%/year) and SEARCH (-6.7%/year) for the same period (Figure 2).

Compared to the observations, the default GEOS-Chem model predicts a steeper decreasing trend of OA mass during 2000-2013 (Figure 1). Modeling results are averaged over the domain [29°~37°N, 74°~96°W] excluding ocean grid cells (Figure S1). The 2000-2013 JJA-averaged

OA from the default model is 6.7 μg/m^3, higher than OA from IMPROVE and SEARCH. Modeled total OA mass decreases at a rate of 4.9%/year, about 1.9 (1.6) times faster than IMPROVE (SEARCH) OA (student's t-test $p<0.001$). By sampling the model results at the locations of the IMPROVE and SEARCH sites, the modeled summertime OA has an average of 6.9 μg/m^3 and a trend of 5.0%/year, similar to the model results averaged over the whole southeast US domain. For simplicity, we show only the domain-averaged model results in all figures and analysis. The strong reduction in total OA mass is dominated by aqueous SOA, especially through reactive uptake of IEPOX, with no decreasing trend in other components (Figure 1). The contribution of IEPOX-SOA to total OA mass decreases from 61% in the early 2000s to 28% in 2013. The simulated IEPOX-SOA in 2013 compares well with previous field studies which suggested that IEPOX-SOA contributed to 18~40% in southeast US sites in summer 2013 (Budisulistiorini et al., 2016; Xu et al., 2015b).

A main constraint comes from the MMV of OA in the southeast US. IMPROVE and SEARCH OA observations show little variability among June, July and August, despite large MMV of sulfate in early 2000s (Figure 2A). We find similar behavior from another observation network, CSN. The discontinuity in OA trend in the CSN network is due to different protocols applied (Figure S2). Within sites using the same protocol, there are no systematic monthly differences, which agrees with IMPROVE and SEARCH. In contrast, modeled OA displays large MMV between June, July and August from 2000 to 2008, where OA in July and August is 1~3 times of June values (Figure 2A). Such large MMV is dominated by aqueous SOA, especially from the reactive uptake of IEPOX. Prior to 2008, the simulated IEPOX-SOA alone can be up to a factor 2 higher than the observed total OA (Figure 2). The other components including POA and dry

SOA (including terpene-SOA and Anthropogenic SOA) formed through partitioning together have low concentrations and small MMV. The default model well captures the variability of observed sulfate (Figure 2A), with an average of 3.8 μg/m^3 and a trend of -6.9%/year, as compared to -6.9%/year (average concentration 4.2 μg/m^3) from IMPROVE and -6.7%/year (average concentration 4.3 μg/m^3) from SEARCH.

The large MMV in the model suggests a much stronger modeled OA dependence on sulfate than observations. In 2000-2004, changes in modeled sulfate from June to July and/or August correspond to large MMV of modeled OA mass. In contrast, little MMV is found in observed OA mass during the same months despite large MMV in observed sulfate (Figure 2A). From a linear regression analysis using all monthly data in 2000-2013, the OA-to-sulfate regression slope is m=0.29 (r^2=0.25) from IMPROVE, m=0.51 (r^2=0.43) from SEARCH, and m=1.87 (r^2=0.57) from the default model, even though the default model well captures the magnitude, trend, and monthly variability of observed sulfate. In summary, simulated total OA mass in the standard GEOS-Chem model, dominated by IEPOX-SOA, has a steeper decreasing trend from 2000 to 2013 than the observations, and has a large MMV indicating strong dependence on sulfate.

3.2 What controls the modeled IEPOX-SOA variability?

The strong dependence of IEPOX-SOA on sulfate is well-established by laboratory and field work: wet sulfate particles provide the surface and volume of liquid media for IEPOX reactive uptake (Budisulistiorini et al., 2017; Eddingsaas et al., 2010; Riva et al., 2016; Xu et al., 2015b, 2016), and serve as nucleophiles for nucleophilic addition to form organosulfates (Nguyen et al.,

2014; Surratt et al., 2007b). Sulfate (SO_4^{2-}), together with ammonium (NH_4^+), nitrate (NO_3^-) and other ions, regulates proton (H^+) activity (a_{H^+}) that can catalyze the ring-opening of epoxide group leading to the formation of IEPOX-SOA (Gaston et al., 2014; Pye et al., 2013; Surratt et al., 2007a). However, some recent studies suggest that IEPOX-SOA is not well correlated with aerosol acidity estimated from thermodynamic models (Budisulistiorini et al., 2015; Lin et al., 2013; Xu et al., 2015b), although the lack of direct measurements of aerosol acidity may be a limitation. We use the GEOS-Chem model here to examine the simulated IEPOX-SOA dependence on sulfate, aerosol acidity, and emissions of isoprene which produce IEPOX at high yields under low-NO_x conditions (Paulot et al., 2009). Temperature impacts the formation of IEPOX-SOA mainly through regulating isoprene emissions but does not influence partitioning as IEPOX-SOA is treated as non-volatile in GEOS-Chem. Therefore, temperature is not examined as another driver in addition to isoprene emissions. We do not treat aerosol water as an independent driver because the dilution effect of aerosol water is implicitly considered in the inorganic sulfate-ammonium-nitrate aerosol volume and acidity calculation, and studies have shown that particle water is not a limiting factor unless the particle is purely dry (Nguyen et al., 2014; Riva et al., 2016; Xu et al., 2015b) which is rare in summertime in the southeast US.

We find that the large MMV of OA in the model is mainly driven by sulfate concentrations and aerosol acidity. Figure 3 shows the standardized monthly surface IEPOX-SOA concentration, sulfate concentration, aerosol H^+ activity and isoprene emission from the default model. For each variable, the monthly gridded data has been first averaged over the southeast US. Then, we calculate the one standard deviation of all monthly data (June, July and August data from 2000 to 2013). Finally, the domain-averaged monthly data has been divided by its standard deviation, so

the variables are standardized to be unitless and their variability can be compared directly. Prior to 2008, IEPOX-SOA production is largely enhanced by abundant sulfate (Gaston et al., 2014). Due to this high level of sulfate (about >4 $\mu g/m^3$), the modeled aerosol acidity becomes particularly sensitive to variations in NH_3 emissions. The default NH_3 emissions from NEI11v1 suggest no significant long-term trend from 2000 to 2013. In general, ammonium aerosol is strongly correlated with sulfate and has a similar declining trend as sulfate (Silvern et al., 2017). However, the NH_3 emissions in August are about 25% lower than in June and July (Figure S4). As a result, in August before 2008, the aerosol NH_4^+/SO_4^{2-} ratio is smaller (Figure S4) and a_{H+} is up to 3 times higher than June (Figure 4B), leading to high production of IEPOX-SOA in August. Both sulfate and aerosol acidity appear to be the dominant contributors to MMV of OA during this period. After 2008, IEPOX-SOA formation is substantially suppressed, due to small SO_2 emissions and low modeled aerosol acidity a_{H+} with small monthly variability. Isoprene emissions also contribute to the month-to-month and interannual OA variability in the model.

The multivariate linear regression analysis of IEPOX-SOA quantitatively determines the relative importance of its three drivers in the model. Using all monthly data in 2000-2013, the standardized regression coefficients (β) associated with a_{H+}, sulfate aerosol concentration and isoprene emission are β=0.50 (r^2=0.71), β=0.39 (r^2=0.64) and β=0.34 (r^2=0.18), respectively, suggesting that aerosol acidity is the dominant controlling factor. The three variables together explain 88% of the variability of IEPOX-SOA. Their relative importance changes over time (Table S1). Aerosol acidity strongly correlates with IEPOX-SOA in 2005-2008 (β=0.57, r^2=0.82) but its role becomes much weaker after 2008 (β=0.27, r^2=0.56). Sulfate aerosol is always the first or second most important driver, especially in 2000-2004 (β=0.46, r^2=0.76).

Isoprene emission contributes to the overall interannual variability, for example leading to the relatively low IEPOX-SOA in 2003-2004 and the peaks in 2000, 2006 and 2011 (Figure 3). The high IEPOX-SOA in 2000-2001 and 2005-2007 is a result of high sulfate aerosol, high aerosol acidity due to low NH_3 supply relative to high sulfate, and high isoprene emissions during these periods (Figure 3, Figure 4B).

3.3 Narrowing the gap between model and observation

3.3.1 Coating

Several reasons may lead to the large monthly variations of the modeled OA. The modeled IEPOX-SOA shows a much stronger sensitivity to aerosol acidity than suggested by field observations, which found weak or no correlation between observed IEPOX-SOA and derived aerosol acidity (Budisulistiorini et al., 2015; Lin et al., 2013; Worton et al., 2013; Xu et al., 2015b). Lack of consideration of organic coating effect may provide one possible explanation. In the real atmosphere, inorganic aerosol is generally internally mixed with other organics (Anttila et al., 2006; Murphy et al., 2006). The presence of an organic coating may alter the solubility and diffusion properties at the surface of inorganic particles and diminish further uptake of IEPOX. We implemented a linear coating effect for the IEPOX uptake in a sensitivity simulation 'CT', in which both the magnitude of γ_{IEPOX} and its sensitivity to acidity have been reduced. Figure 4A shows a schematic illustrating the dependence of the γ_{IEPOX} coating effect on acidity a_{H+} and organic mass fraction (χ_{org}). The original γ_{IEPOX} without coating is represented at χ_{org}=0. The orange line in Figure 4A shows the approximate position of JJA-averaged acidity and organic mass fraction in the 'CT' simulation. Adding a coating reduces γ_{IEPOX} by almost half, but the impact on the total reactive uptake rate of IEPOX is partially compensated by the corresponding

increase in particle surface area. The sensitivity of γ_{IEPOX} to acidity has also been reduced especially during the early 2000s (Figure 4A). The CT simulation reduces the southeast US JJA-averaged IEPOX-SOA concentrations by 0.3~1.8 μg/m^3 (Figure 4C).

3.3.2 NH_3 emissions and aerosol acidity

Second, recent studies present contradictory results and explanations on the long-term trend of aerosol acidity in the southeast US (Pye et al., 2020; Silvern et al., 2017; Weber et al., 2016). In this study, we show that the decreasing trend of aerosol acidity from the standard GEOS-Chem model is mainly caused by high acidity in August before 2008, which corresponds to insufficient NH_3 emissions in high sulfate environments. The NEI11v1 inventory is used in the default configuration, in which NH_3 emissions in June and July are 30% higher than in August (Figure S4), but not all NH_3 emission inventories agree with such pattern (Paulot et al., 2014). We did a sensitivity test ('CT_newNH_3') replacing the default US NH_3 emissions from NEI11v1 by a new NH_3 emission product derived from CrIS satellite observations, which has higher emissions and smaller MMV among June, July and August (Figure S4). In the 'CT_newNH_3' simulation, the resulting simulated aerosol acidity is substantially changed in 2000-2008 (Figure 4B). The high acidity (a_{H+}=0.55~0.9 mol/L) in August has been reduced to around 0.2 mol/L and is much closer to June and July values (Figure 3). The results suggest that the fine particles in the southeast US are within a regime where the acidity (a_{H+} in units of mol/L) is sensitive to NH_3 emissions relative to sulfate concentration, though corresponding pH changes are small (pH within 0.5~1.5, Figure S4). Small changes in NH_3 may lead to large changes in a_{H+} especially when sulfate concentrations are high, resulting in high month-to-month variability of the IEPOX uptake. After updating the NH_3 emissions using the satellite-based estimates, the model

simulates a much more stable trend in aerosol acidity from 2000 to 2013 (Figure 4B), consistent with recent thermodynamic modeling studies that suggested steady aerosol acidity despite large reductions in observed sulfate (Pye et al., 2020; Weber et al., 2016).

Due to the high uncertainty associated with the derived NH_3 emission product and acidity calculation (Guo et al., 2015, 2018; Silvern et al., 2017; Song et al., 2018; Tao and Murphy, 2019), we conducted another simulation 'CT_H01' that fix a_{H+} level at 0.1 mol/L when calculating IEPOX uptake rate, corresponding to the predicted a_{H+} value (constrained by observations) during the 2013 SOAS campaign (Weber et al., 2016). The two simulations, CT_newNH_3 and CT_H01, yield similar long-term trends of IEPOX-SOA in the southeast US (Figure S5), and they agree better with the long-term surface OA measurements from IMPROVE and SEARCH than the default model (Figure 4C and 4D). For the SOAS2013 campaign, the CT_H01 scheme simulates an average IEPOX-SOA concentration of 0.74 μg/m^3, similar to 0.81 μg/m^3 in the default model, and agrees well with the two independent Aerosol Mass Spectrometer measurements (0.97 μg/m^3 from obs_GT and 0.68 μg/m^3 from obs_CU, see daily time series in Figure S6). The CT_newNH_3 scheme simulates an average IEPOX-SOA concentration of 0.34 μg/m^3, lower than the observation and the other models by a factor of >2, due to both the simplified coating effect and small aerosol a_{H+} values (a_{H+}<0.1mol/L, Figure 4B). In general, the fixed acidity in the CT_H01 simulation well captures the measured IEPOX-SOA from the SOAS2013 campaign (Figure S6), and improves the modeled total OA mass relative to the observations: The modeled long-term decreasing rate of JJA-average OA from 2000 to 2013 has been reduced from 4.9%/year to 3.2%/year, better compared to the IMPROVE

(1.7%/year) and SEARCH (1.9%/year) observations, but is still higher (Figure 4C). The modeled MMV of OA have also been greatly reduced (Figure 4D).

3.3.3 Relationships between OA and sulfate

The formation of aqueous SOA explicitly depends on sulfate aerosol and aerosol acidity which is also impacted by sulfate. The default model, in which a large fraction of simulated total OA mass is from aqueous SOA (mostly IEPOX-SOA), shows a stronger dependence of total OA on sulfate than the observations (Figure 5). The OA-to-sulfate regression slope calculated using monthly OA and sulfate (averaged from all sites beforehand for each network) is m=1.87 for the default simulation, much higher than m=0.29 from IMPROVE and m=0.51 from SEARCH. Such strong dependence is clearly demonstrated by the MMV of IEPOX-SOA (Figure 2). Adding the coating effect and fixing a_{H^+}=0.1 mol/L substantially reduces the MMV of IEPOX-SOA and the simulated monthly OA-to-sulfate slope (m=1.02).

Despite the model improvement against the observations in terms of OA and IEPOX-SOA magnitude and long-term relationship with sulfate, the CT_H01 scheme needs to be further improved. The rate of OA decreases per year in CT_H01 is about 0.8 times higher than the long-term observations, with modeled MMV still larger than observations in early 2000s (Figure 4D). Recent studies (Riva et al., 2019) suggested that the IEPOX-SOA production per unit mass of sulfate likely increases with decreasing sulfate due to changes in aerosol properties, such as acidity, morphology, phase state and viscosity, as well as formation of organosulfates, suggesting non-linearity between IEPOX-SOA and sulfate (Riva et al., 2019; Zhang et al., 2019a). Further

449 modeling studies with separated IEPOX-SOA species and detailed aerosol properties are needed
450 to achieve a better mechanistic understanding of the dependence of OA on inorganic aerosol.
451

452 # 4. Summary and Discussion

453 Significant reduction of SO_2 emissions, combined with monthly variations of sulfate and NH_3
454 emissions, provide a unique dataset to test the sensitivity of biogenic SOA formation to inorganic
455 species. Observations from two networks (IMPROVE and SEARCH) show a slowly decreasing
456 trend in total OA mass from 2000 to 2013 in the southeast US (-1.7%/year from IMPROVE and -
457 1.9%/year from SEARCH), in contrast to a much faster rate of sulfate reduction (-6.9%/year
458 from IMPROVE and -6.7%/year from SEARCH). The standard version of GEOS-Chem model
459 was able to reproduce the long-term trend of sulfate (-6.7%/year), but with a faster decrease of
460 OA (-4.9%/year) and larger interannual variability.
461

462 The MMV of total OA mass during summers provides a novel observational constraint on SOA
463 formation mechanism. Remarkably, we find little MMV of OA from all three surface networks
464 (IMPROVE, SEARCH and CSN) during summer months in 2000-2013, despite larger MMV in
465 sulfate and NH_3 emissions. This is in contrast to the standard version of the GEOS-Chem model,
466 which shows a much larger MMV of OA during 2000-2008. Large MMV of OA in the standard
467 model is mainly due to the high sensitivity of modeled IEPOX-SOA to sulfate and aerosol
468 acidity (and NH_3 emissions) when sulfate aerosol is abundant. The resulting strong correlation
469 between OA and sulfate also appears to be at odds with long-term observations (Figure 5).
470 Incorporating a coating effect for IEPOX uptake and fixing aerosol acidity, have together

471 improved the model performance in terms of OA trend, variability and the relationship between
472 OA and sulfate, though further improvement is needed.
473
474 There are many uncertainties associated with the calculation of IEPOX-SOA formation. In the
475 default scheme, the Henry's law constant for IEPOX uptake was tuned using measurements from
476 the SOAS2013 campaign and was found to be 1.7×10^7 M/atm, 10 times smaller than suggested
477 by Gaston et al. (2014) based on laboratory experiments and about half of the suggested value
478 (3×10^7 M/atm) in some other studies (Budisulistiorini et al., 2017; Nguyen et al., 2014; Pye et
479 al., 2017; Woo and McNeill, 2015; Zhang et al., 2018b). The default simulation agrees well with
480 surface IEPOX-SOA data from SOAS2013 and SEAC4RS 2013 aircraft campaigns (Marais et
481 al., 2016) but overestimates OA magnitude and MMV against long-term observations from
482 IMPROVE and SEARCH. The CT_newNH_3 simulation reproduces the long-term OA trend but
483 underestimates IEPOX-SOA by a factor of 2 against SOAS 2013. The coating effect may be
484 stronger than used here, as Gaston et al. (2014) used a low viscosity organic material in the
485 experiments. The NH_3 emissions (which are critical for the calculation of aerosol acidity) are
486 highly uncertain (Dammers et al., 2019), and the acidity calculation is further complicated by
487 non-volatile cations (Guo et al., 2018) and meteorological conditions (Guo et al., 2015; Tao and
488 Murphy, 2019). Uncertainties are also associated with the volatility of IEPOX-SOA. Some
489 studies suggested a large fraction of IEPOX-SOA compounds (e.g. 2-methyltetrol) are semi-
490 volatile and can re-evaporate back into gas-phase (Ambro et al., 2019; Isaacman-VanWertz et
491 al., 2016), while other studies suggest IEPOX-SOA products are mostly nonvolatile or low
492 volatility (Hu et al., 2016; Lopez-Hilfiker et al., 2016). As multiple parameters may be tuned in
493 the model to fit observations, further laboratory, field and modeling studies are needed to

integrate Henry's law constant, IEPOX-SOA yields, volatility, coating effect and acidity dependence for a better mechanistic understanding. The CT_H01 scheme lacks mechanical representation of detailed aerosol properties like phase state, acidity, viscosity and morphology, but reasonably captures both the OA and IEPOX-SOA magnitude (compared to both the three filter measurement networks and the SOAS2013 campaign), long-term variability and relationship with sulfate (Figure 4, 5, S6), therefore may serve as a simplified representation for climate models. Simulations in this study are conducted at a horizontal resolution of 2°×2.5°, which is comparable to most global climate models. However, as shown by Yu et al. (2016), from coarse to fine horizontal resolution, there will be a shift from low-NO_x to high-NO_x pathway for isoprene oxidation. Therefore, using a fine resolution may reduce the production of IEPOX and IEPOX-SOA, which needs further investigation. For all kinds of models, long-term filter-based measurements, especially intraseasonal MMV, are important observational constraints that should be considered in model development.

Even with our improved model, the rate of OA decrease per year is still 0.8 times higher the long-term observations, and still shows a higher MMV than observations particularly in early 2000s (Figure 4D). Such discrepancies may suggest a more important role of SOA pathways that are less dependent on inorganic aerosol, such as terpene-SOA formed by reversible gas-aerosol partitioning. Terpene-SOA is included in GEOS-Chem (yellow color in Figure 1), and contributes to 8~24% of total OA, which might be underestimated compared to recent field studies. Xu et al. (2015a) finds a large MMV in IEPOX-SOA, but the less-oxidized oxygenated OA (LO-OOA, an indicator for freshly-formed monoterpene SOA) and the more-oxidized oxygenated OA (MO-OOA, also likely from biogenic sources) have little MMV in summer

517 months, and they contribute to more than 50% of total OA mass in the southeast US (Xu et al.,
518 2018). The important role of monoterpenes SOA is also confirmed by molecular level
519 characterization of organic aerosols (Zhang et al., 2018a). Other pathways may contribute to
520 SOA to some extent and may add to the predicted SOA formed by partitioning, including
521 biogenic SOA from auto-oxidation (Bianchi et al., 2019; Pye et al., 2019), in-cloud SOA
522 formation that may be less dependent on acidity than aqueous SOA (Tsui et al., 2019), a small
523 but underestimated contribution of anthropogenic SOA (Schroder et al., 2018; Shah et al., 2019),
524 and other possible mechanisms (Schwantes et al., 2019). Further quantifying the relative
525 importance of the different pathways will allow a more accurate quantification of the
526 anthropogenic influence on biogenic SOA and the associated radiative forcing.
527
528

Data availability

The observational datasets from long-term filter measurement networks IMPROVE and CSN are available at http://views.cira.colostate.edu/fed/QueryWizard/Default.aspx. The SEARCH observational datasets are available by contacting E. Edgerton. The model code and modeling results are available by contacting Y. Zheng and J. Mao.

Acknowledgement

YZ and JM acknowledge funding from NOAA NA18OAR4310114. HC and DKJ recognize support from NASA 80NSSC18K0689. WH and JLJ acknowledge funding from NSF AGS-1822664. EAM acknowledges funding from NERC/EPSRC (award number EP/R513465/1). The authors acknowledge the Electric Power Research Institute (EPRI) and Southern Company for support of the SEARCH network and Atmospheric Research & Analysis. IMPROVE and CSN data are accessed from the Federal Land Manger Environmental Database. YZ thanks helpful discussions with Arlene M. Fiore, Róisín Commane and V. Faye McNeill.

Author Contributions:

Y.Z. and J.M. designed the research, performed the simulations and conducted the analysis. J.A.T. and E.M.M. provided guidance on aerosol coating parameterization. H.C. and D.K.H. provided the CrIS-derived NH_3 emission. N.L.N, W.H. and J.L.J. provided data from the SOAS2013 field campaign. E.E. provided data from the SEARCH network. Y.Z. wrote the paper with all coauthors providing input.

Competing interests

The authors declare no competing interests.

Additional information

Correspondence and material requests should be addressed to Y. Zheng and J. Mao.

Reference:

Ambro, E. L., Schobesberger, S., Gaston, C. J., Lopez-Hilfiker, F. D., Lee, B. H., Liu, J., Zelenyuk, A., Bell, D., Cappa, C. D., Helgestad, T., Li, Z., Guenther, A., Wang, J., Wise, M., Caylor, R., Surratt, J. D., Riedel, T., Hyttinen, N., Salo, V.-T., Hasan, G., Kurtén, T., Shilling, J. E. and Thornton, J. A.: Chamber-based insights into the factors controlling IEPOX SOA yield, composition, and volatility, Atmos. Chem. Phys., 19, 11253–11265, doi:10.5194/acp-2019-271, 2019.

Anttila, T., Kiendler-Scharr, A., Tillmann, R. and Mentel, T. F.: On the reactive uptake of gaseous compounds by organic-coated aqueous aerosols: Theoretical analysis and application to the heterogeneous hydrolysis of N2O5, J. Phys. Chem. A, 110(35), 10435–10443, doi:10.1021/jp062403c, 2006.

Attwood, A. R., Washenfelder, R. A., Brock, C. A., Hu, W., Baumann, K., Campuzano-Jost, P., Day, D. A., Edgerton, E. S., Murphy, D. M., Palm, B. B., McComiskey, A., Wagner, N. L., De Sá, S. S., Ortega, A., Martin, S. T., Jimenez, J. L. and Brown, S. S.: Trends in sulfate and organic aerosol mass in the Southeast U.S.: Impact on aerosol optical depth and radiative forcing, Geophys. Res. Lett., 41, 7701–7709, doi:10.1002/2014GL061669, 2014.

Bey, I., Jacob, D. J., Yantosca, R. M., Logan, J. A., Field, B. D., Fiore, A. M., Li, Q.-B., Liu, H.-Y., Mickley, L. J. and Schultz, M. G.: Global Modeling of Tropospheric Chemistry with Assimilated Meteorology: Model Description and Evaluation, J. Geophys. Res., 106, 73–95, doi:10.1029/2001JD000807, 2001.

Bianchi, F., Kurtén, T., Riva, M., Mohr, C., Rissanen, M. P., Roldin, P., Berndt, T., Crounse, J. D., Wennberg, P. O., Mentel, T. F., Wildt, J., Junninen, H., Jokinen, T., Kulmala, M., Worsnop, D. R., Thornton, J. A., Donahue, N., Kjaergaard, H. G. and Ehn, M.: Highly Oxygenated Organic Molecules (HOM) from Gas-Phase Autoxidation Involving Peroxy Radicals: A Key Contributor to Atmospheric Aerosol, Chem. Rev., 119(6), 3472–3509, doi:10.1021/acs.chemrev.8b00395, 2019.

Blanchard, C. L., Hidy, G. M., Shaw, S., Baumann, K. and Edgerton, E. S.: Effects of emission reductions on organic aerosol in the southeastern United States, Atmos. Chem. Phys., 16, 215–238, doi:10.5194/acp-16-215-2016, 2016.

Budisulistiorini, S. H., Li, X., Bairai, S. T., Renfro, J., Liu, Y., Liu, Y. J., McKinney, K. A., Martin, S. T., McNeill, V. F., Pye, H. O. T., Nenes, A., Neff, M. E., Stone, E. A., Mueller, S., Knote, C., Shaw, S. L., Zhang, Z., Gold, A. and Surratt, J. D.: Examining the effects of anthropogenic emissions on isoprene-derived secondary organic aerosol formation during the 2013 Southern Oxidant and Aerosol Study (SOAS) at the Look Rock, Tennessee ground site, Atmos. Chem. Phys., 15(15), 8871–8888, doi:10.5194/acp-15-8871-2015, 2015.

Budisulistiorini, S. H., Baumann, K., Edgerton, E. S., Bairai, S. T., Mueller, S., Shaw, S. L., Knipping, E. M., Gold, A. and Surratt, J. D.: Seasonal characterization of submicron aerosol chemical composition and organic aerosol sources in the southeastern United States: Atlanta, Georgia,and Look Rock, Tennessee, Atmos. Chem. Phys., 16(8), 5171–5189, doi:10.5194/acp-16-5171-2016, 2016.

Budisulistiorini, S. H., Nenes, A., Carlton, A. G., Surratt, J. D., McNeill, V. F. and Pye, H. O. T.: Simulating Aqueous-Phase Isoprene-Epoxydiol (IEPOX) Secondary Organic Aerosol Production during the 2013 Southern Oxidant and Aerosol Study (SOAS), Environ. Sci. Technol., 51(9), 5026–5034, doi:10.1021/acs.est.6b05750, 2017.

Butler, T., Vermeylen, F., Lehmann, C. M., Likens, G. E. and Puchalski, M.: Increasing ammonia concentration trends in large regions of the USA derived from the NADP/AMoN

network, Atmos. Environ., 146(3), 132–140, doi:10.1016/j.atmosenv.2016.06.033, 2016.
Cao, H., Henze, D. K., Shephard, M. W., Dammers, E., Cady-Pereira, K., Alvarado, M. J., Lonsdale, C. R., Luo, G., Yu, F., Zhu, L., Danielson, C. G. and Edgerton, E. S.: Inverse modeling of NH3 sources using CrIS remote sensing measurements, Environ. Res. Lett., in press, doi:https://doi.org/10.1088/1748-9326/abb5cc, 2020.
Carlton, A. G., Pinder, R. W., Bhave, P. V. and Pouliot, G. A.: To what extent can biogenic SOA be controlled?, Environ. Sci. Technol., 44(9), 3376–3380, doi:10.1021/es903506b, 2010.
Dammers, E., McLinden, C. A., Griffin, D., Shephard, M. W., Van Der Graaf, S., Lutsch, E., Schaap, M., Gainairu-Matz, Y., Fioletov, V., Van Damme, M., Whitburn, S., Clarisse, L., Cady-Pereira, K., Clerbaux, C., Francois Coheur, P. and Erisman, J. W.: NH3 emissions from large point sources derived from CrIS and IASI satellite observations, Atmos. Chem. Phys., 19(19), 12261–12293, doi:10.5194/acp-19-12261-2019, 2019.
Donahue, N. M., Robinson, a. L., Stanier, C. O. and Pandis, S. N.: Coupled partitioning, dilution, and chemical aging of semivolatile organics, Environ. Sci. Technol., 40(8), 2635–2643, doi:10.1021/es052297c, 2006.
Eddingsaas, N. C., Vandervelde, D. G. and Wennberg, P. O.: Kinetics and products of the acid-catalyzed ring-opening of atmospherically relevant butyl epoxy alcohols, J. Phys. Chem. A, 114, 8106–8113, doi:10.1021/jp103907c, 2010.
Edgerton, E. S., Hartsell, B. E., Saylor, R. D., Jansen, J. J., Hansen, D. A. and Hidy, G. M.: The southeastern aerosol research and characterization study: Part II. Filter-based measurements of fine and coarse particulate matter mass and composition, J. Air Waste Manag. Assoc., 55(10), 1527–1542, doi:10.1080/10473289.2005.10464744, 2005.
EPA: The benefits and costs of the clean air act from 1990-2020, in Better Air: Benefits and Costs of the Clean Air Act., 2011.
Ervens, B., Turpin, B. J. and Weber, R. J.: Secondary organic aerosol formation in cloud droplets and aqueous particles (aqSOA): A review of laboratory, field and model studies, Atmos. Chem. Phys., 11(21), 11069–11102, doi:10.5194/acp-11-11069-2011, 2011.
Fisher, J. A., Jacob, D. J., Travis, K. R., Kim, P. S., Marais, E. A., Miller, C. C., Yu, K., Zhu, L., Yantosca, R. M., Sulprizio, M. P., Mao, J., Wennberg, P. O., Crounse, J. D., Teng, A. P., Nguyen, T. B., Clair, J. M. S., Cohen, R. C., Romer, P., Nault, B. A., Wooldridge, P. J., Jimenez, J. L., Campuzano-Jost, P., Day, D. A., Hu, W., Shepson, P. B., Xiong, F., Blake, D. R., Goldstein, A. H., Misztal, P. K., Hanisco, T. F., Wolfe, G. M., Ryerson, T. B., Wisthaler, A. and Mikoviny, T.: Organic nitrate chemistry and its implications for nitrogen budgets in an isoprene- and monoterpene-rich atmosphere: Constraints from aircraft (SEAC4RS) and ground-based (SOAS) observations in the Southeast US, Atmos. Chem. Phys., 16(9), 5969–5991, doi:10.5194/acp-16-5969-2016, 2016.
Fountoukis, C. and Nenes, A.: ISORROPIA II: a computationally efficient thermodynamic equilibrium model for K+-Ca2+-Mg2+-NH4+-Na+-SO42--NO3--Cl−-H2O aerosols, Atmos. Chem. Phys, 7, 4639–4659, doi:10.5194/acp-7-4639-2007, 2007.
Fu, T. M., Jacob, D. J., Wittrock, F., Burrows, J. P., Vrekoussis, M. and Henze, D. K.: Global budgets of atmospheric glyoxal and methylglyoxal, and implications for formation of secondary organic aerosols, J. Geophys. Res. Atmos., doi:10.1029/2007JD009505, 2008.
Gaston, C. J., Riedel, T. P., Zhang, Z., Gold, A., Surratt, J. D. and Thornton, J. A.: Reactive uptake of an isoprene-derived epoxydiol to submicron aerosol particles, Environ. Sci. Technol., 48(19), 11178–11186, doi:10.1021/es5034266, 2014.
Guenther, A. B., Karl, T., Harley, P., Wiedinmyer, C., Palmer, P. I. and Geron, C.: Estimates of

global terrestrial isoprene emissions using MEGAN (Model of Emissions of Gases and Aerosols from Nature), Atmos. Chem. Phys., 6, 3181–3210, doi:doi:10.5194/acp-6-3181-2006, 2006.
Guenther, A. B., Jiang, X., Heald, C. L., Sakulyanontvittaya, T., Duhl, T., Emmons, L. K. and Wang, X.: The model of emissions of gases and aerosols from nature version 2.1 (MEGAN2.1): An extended and updated framework for modeling biogenic emissions, Geosci. Model Dev., 5, 1471–1492, doi:10.5194/gmd-5-1471-2012, 2012.
Guo, H., Xu, L., Bougiatioti, A., Cerully, K. M., Capps, S. L., Hite, J. R., Carlton, A. G., Lee, S. H., Bergin, M. H., Ng, N. L., Nenes, A. and Weber, R. J.: Fine-particle water and pH in the southeastern United States, Atmos. Chem. Phys., 15(9), 5211–5228, doi:10.5194/acp-15-5211-2015, 2015.
Guo, H., Nenes, A. and Weber, R. J.: The underappreciated role of nonvolatile cations in aerosol ammonium-sulfate molar ratios, Atmos. Chem. Phys., 18(23), 17307–17323, doi:10.5194/acp-18-17307-2018, 2018.
Hayes, P. L., Carlton, A. G., Baker, K. R., Ahmadov, R., Washenfelder, R. A., Alvarez, S., Rappenglück, B., Gilman, J. B., Kuster, W. C., De Gouw, J. A., Zotter, P., Prévôt, A. S. H., Szidat, S., Kleindienst, T. E., Offenberg, J. H., Ma, P. K. and Jimenez, J. L.: Modeling the formation and aging of secondary organic aerosols in Los Angeles during CalNex 2010, Atmos. Chem. Phys., 15(10), 5773–5801, doi:10.5194/acp-15-5773-2015, 2015.
Henze, D. K., Hakami, A. and Seinfeld, J. H.: Development of the adjoint of GEOS-Chem, Atmos. Chem. Phys., 7(9), 2413–2433, doi:10.5194/acp-7-2413-2007, 2007.
Hidy, G. M., Blanchard, C. L., Baumann, K., Edgerton, E., Tanenbaum, S., Shaw, S., Knipping, E., Tombach, I., Jansen, J. and Walters, J.: Chemical climatology of the southeastern United States, 1999-2013, Atmos. Chem. Phys., 14(21), 11893–11914, doi:10.5194/acp-14-11893-2014, 2014.
Hodshire, A. L., Akherati, A., Alvarado, M. J., Brown-Steiner, B., Jathar, S. H., Jimenez, J. L., Kreidenweis, S. M., Lonsdale, C. R., Onasch, T. B., Ortega, A. M. and Pierce, J. R.: Aging Effects on Biomass Burning Aerosol Mass and Composition: A Critical Review of Field and Laboratory Studies, Environ. Sci. Technol., 53(17), 10007–10022, doi:10.1021/acs.est.9b02588, 2019.
Hu, W., Palm, B. B., Day, D. A., Campuzano-Jost, P., Krechmer, J. E., Peng, Z., De Sa Suzane, S., Martin, S. T., Alexander, M. L., Baumann, K., Hacker, L., Kiendler-Scharr, A., Koss, A. R., De Gouw, J. A., Goldstein, A. H., Seco, R., Sjostedt, S. J., Park, J. H., Guenther, A. B., Kim, S., Canonaco, F., Prévôt, A. S. H., Brune, W. H. and Jimenez, J. L.: Volatility and lifetime against OH heterogeneous reaction of ambient isoprene-epoxydiols-derived secondary organic aerosol (IEPOX-SOA), Atmos. Chem. Phys., 16(18), 11563–11580, doi:10.5194/acp-16-11563-2016, 2016.
Hu, W. W., Campuzano-Jost, P., Palm, B. B., Day, D. A., Ortega, A. M., Hayes, P. L., Krechmer, J. E., Chen, Q., Kuwata, M., Liu, Y. J., De Sá, S. S., McKinney, K., Martin, S. T., Hu, M., Budisulistiorini, S. H., Riva, M., Surratt, J. D., St. Clair, J. M., Isaacman-Van Wertz, G., Yee, L. D., Goldstein, A. H., Carbone, S., Brito, J., Artaxo, P., De Gouw, J. A., Koss, A., Wisthaler, A., Mikoviny, T., Karl, T., Kaser, L., Jud, W., Hansel, A., Docherty, K. S., Alexander, M. L., Robinson, N. H., Coe, H., Allan, J. D., Canagaratna, M. R., Paulot, F. and Jimenez, J. L.: Characterization of a real-time tracer for isoprene epoxydiols-derived secondary organic aerosol (IEPOX-SOA) from aerosol mass spectrometer measurements, Atmos. Chem. Phys., 15(20), 11807–11833, doi:10.5194/acp-15-11807-2015, 2015.
Isaacman-VanWertz, G., Yee, L. D., Kreisberg, N. M., Wernis, R., Moss, J. A., Hering, S. V., De

Sá, S. S., Martin, S. T., Alexander, M. L., Palm, B. B., Hu, W., Campuzano-Jost, P., Day, D. A., Jimenez, J. L., Riva, M., Surratt, J. D., Viegas, J., Manzi, A., Edgerton, E., Baumann, K., Souza, R., Artaxo, P. and Goldstein, A. H.: Ambient Gas-Particle Partitioning of Tracers for Biogenic Oxidation, Environ. Sci. Technol., 50(18), 9952–9962, doi:10.1021/acs.est.6b01674, 2016.
Janssens-Maenhout, G., Crippa, M., Guizzardi, D., Dentener, F., Muntean, M., Pouliot, G., Keating, T., Zhang, Q., Kurokawa, J., Wankmüller, R., Denier Van Der Gon, H., Kuenen, J. J. P., Klimont, Z., Frost, G., Darras, S., Koffi, B. and Li, M.: HTAP-v2.2: A mosaic of regional and global emission grid maps for 2008 and 2010 to study hemispheric transport of air pollution, Atmos. Chem. Phys., 15(19), 11411–11432, doi:10.5194/acp-15-11411-2015, 2015.
Jimenez, J. L., Canagaratna, M. R., Donahue, N. M., Prevot, A. S. H., Zhang, Q., Kroll, J. H., DeCarlo, P. F., Allan, J. D., Coe, H., Ng, N. L., Aiken, A. C., Docherty, K. S., Ulbrich, I. M., Grieshop, A. P., Robinson, A. L., Duplissy, J., Smith, J. D., Wilson, K. R., Lanz, V. A., Hueglin, C., Sun, Y. L., Tian, J., Laaksonen, A., Raatikainen, T., Rautiainen, J., Vaattovaara, P., Ehn, M., Kulmala, M., Tomlinson, J. M., Collins, D. R., Cubison, M. J., Dunlea, E. J., Huffman, J. A., Onasch, T. B., Alfarra, M. R., Williams, P. I., Bower, K., Kondo, Y., Schneider, J., Drewnick, F., Borrmann, S., Weimer, S., Demerjian, K., Salcedo, D., Cottrell, L., Griffin, R., Takami, A., Miyoshi, T., Hatakeyama, S., Shimono, A., Sun, J. Y., Zhang, Y. M., Dzepina, K., Kimmel, J. R., Sueper, D., Jayne, J. T., Herndon, S. C., Trimborn, A. M., Williams, L. R., Wood, E. C., Middlebrook, A. M., Kolb, C. E., Baltensperger, U. and Worsnop, D. R.: Evolution of organic aerosols in the atmosphere, Science (80-.)., 326(5959), 1525–1529, doi:10.1126/science.1180353, 2009.
Jo, D. S., Hodzic, A., Emmons, L. K., Marais, E. A., Peng, Z., Nault, B. A., Hu, W., Campuzano-Jost, P. and Jimenez, J. L.: A simplified parameterization of isoprene-epoxydiol-derived secondary organic aerosol (IEPOX-SOA) for global chemistry and climate models: A case study with GEOS-Chem v11-02-rc, Geosci. Model Dev., 12(7), 2983–3000, doi:10.5194/gmd-12-2983-2019, 2019.
Kiendler-Scharr, A., Mensah, A. A., Friese, E., Topping, D., Nemitz, E., Prevot, A. S. H., Äijälä, M., Allan, J., Canonaco, F., Canagaratna, M., Carbone, S., Crippa, M., Dall Osto, M., Day, D. A., De Carlo, P., Di Marco, C. F., Elbern, H., Eriksson, A., Freney, E., Hao, L., Herrmann, H., Hildebrandt, L., Hillamo, R., Jimenez, J. L., Laaksonen, A., McFiggans, G., Mohr, C., O'Dowd, C., Otjes, R., Ovadnevaite, J., Pandis, S. N., Poulain, L., Schlag, P., Sellegri, K., Swietlicki, E., Tiitta, P., Vermeulen, A., Wahner, A., Worsnop, D. and Wu, H. C.: Ubiquity of organic nitrates from nighttime chemistry in the European submicron aerosol, Geophys. Res. Lett., 43(14), 7735–7744, doi:10.1002/2016GL069239, 2016.
Kim, P. S., Jacob, D. J., Fisher, J. A., Travis, K., Yu, K., Zhu, L., Yantosca, R. M., Sulprizio, M. P., Jimenez, J. L., Campuzano-Jost, P., Froyd, K. D., Liao, J., Hair, J. W., Fenn, M. A., Butler, C. F., Wagner, N. L., Gordon, T. D., Welti, A., Wennberg, P. O., Crounse, J. D., St. Clair, J. M., Teng, A. P., Millet, D. B., Schwarz, J. P., Markovic, M. Z. and Perring, A. E.: Sources, seasonality, and trends of Southeast US aerosol: An integrated analysis of surface, aircraft, and satellite observations with the GEOS-Chem chemical transport model, Atmos. Chem. Phys. Discuss., 15(13), 17651–17709, doi:10.5194/acpd-15-17651-2015, 2015.
Kroll, J. H., Ng, N. L., Murphy, S. M., Flagan, R. C. and Seinfeld, J. H.: Secondary organic aerosol formation from isoprene photooxidation under high-NOx conditions, Geophys. Res. Lett., 32(x), 1–4, doi:10.1029/2005GL023637, 2005.
Kroll, J. H., Ng, N. L., Murphy, S. M., Flagan, R. C. and Seinfeld, J. H.: Secondary organic aerosol formation from isoprene photooxidation, Environ. Sci. Technol., 40(3), 1869–1877,

741 doi:10.1021/es0524301, 2006.
742 Li, J., Mao, J., Min, K. E., Washenfelder, R. A., Brown, S. S., Kaiser, J., Keutsch, F. N.,
743 Volkamer, R., Wolfe, G. M., Hanisco, T. F., Pollack, I. B., Ryerson, T. B., Graus, M., Gilman, J.
744 B., Lerner, B. M., Warneke, C., de Gouw, J. A., Middlebrook, A. M., Liao, J., Welti, A.,
745 Henderson, B. H., Faye McNeill, V., Hall, S. R., Ullmann, K., Donner, L. J., Paulot, F. and
746 Horowitz, L. W.: Observational constraints on glyoxal production from isoprene oxidation and
747 its contribution to organic aerosol over the Southeast United States, J. Geophys. Res.,
748 doi:10.1002/2016JD025331, 2016.
749 Li, J., Mao, J., Fiore, A. M., Cohen, R. C., Crounse, J. D., Teng, A. P., Wennberg, P. O., Lee, B.
750 H., Lopez-Hilfiker, F. D., Thornton, J. A., Peischl, J., Pollack, I. B., Ryerson, T. B., Veres, P.,
751 Roberts, J. M., Neuman, J. A., Nowak, J. B., Wolfe, G. M., Hanisco, T. F., Fried, A., Singh, H.
752 B., Dibb, J., Paulot, F. and Horowitz, L. W.: Decadal changes in summertime reactive oxidized
753 nitrogen and surface ozone over the Southeast United States, Atmos. Chem. Phys., 18(3), 2341–
754 2361, doi:10.5194/acp-18-2341-2018, 2018.
755 Li, Y., Day, D. A., Stark, H., Jimenez, J. L. and Shiraiwa, M.: Predictions of the glass transition
756 temperature and viscosity of organic aerosols from volatility distributions, Atmos. Chem. Phys.,
757 20(13), 8103–8122, doi:10.5194/acp-20-8103-2020, 2020.
758 Liggio, J., Li, S. M. and McLaren, R.: Reactive uptake of glyoxal by particulate matter, J.
759 Geophys. Res. D Atmos., 110(10), 1–13, doi:10.1029/2004JD005113, 2005.
760 Lin, Y. H., Knipping, E. M., Edgerton, E. S., Shaw, S. L. and Surratt, J. D.: Investigating the
761 influences of SO2 and NH3 levels on isoprene-derived secondary organic aerosol formation
762 using conditional sampling approaches, Atmos. Chem. Phys., 13(16), 8457–8470,
763 doi:10.5194/acp-13-8457-2013, 2013.
764 Lopez-Hilfiker, F. D., Mohr, C., D'Ambro, E. L., Lutz, A., Riedel, T. P., Gaston, C. J., Iyer, S.,
765 Zhang, Z., Gold, A., Surratt, J. D., Lee, B. H., Kurten, T., Hu, W. W., Jimenez, J., Hallquist, M.
766 and Thornton, J. A.: Molecular Composition and Volatility of Organic Aerosol in the
767 Southeastern U.S.: Implications for IEPOX Derived SOA, Environ. Sci. Technol., 50(5), 2200–
768 2209, doi:10.1021/acs.est.5b04769, 2016.
769 Malm, W. C., Schichtel, B. A., Hand, J. L. and Collett, J. L.: Concurrent Temporal and Spatial
770 Trends in Sulfate and Organic Mass Concentrations Measured in the IMPROVE Monitoring
771 Program, J. Geophys. Res. Atmos., 122(19), 10462–10476, doi:10.1002/2017JD026865, 2017.
772 Mao, J., Paulot, F., Jacob, D. J., Cohen, R. C., Crounse, J. D., Wennberg, P. O., Keller, C. A.,
773 Hudman, R. C., Barkley, M. P. and Horowitz, L. W.: Ozone and organic nitrates over the eastern
774 United States: Sensitivity to isoprene chemistry, J. Geophys. Res. Atmos., 118(19), 11256–
775 11268, doi:10.1002/jgrd.50817, 2013.
776 Mao, J., Carlton, A., Cohen, R. C., Brune, W. H., Brown, S. S., Wolfe, G. M., Jimenez, J. L.,
777 Pye, H. O. T., Lee Ng, N., Xu, L., Faye McNeill, V., Tsigaridis, K., McDonald, B. C., Warneke,
778 C., Guenther, A., Alvarado, M. J., De Gouw, J., Mickley, L. J., Leibensperger, E. M., Mathur,
779 R., Nolte, C. G., Portmann, R. W., Unger, N., Tosca, M. and Horowitz, L. W.: Southeast
780 Atmosphere Studies: Learning from model-observation syntheses, Atmos. Chem. Phys., 18(4),
781 2615–2651, doi:10.5194/acp-18-2615-2018, 2018.
782 Marais, E. A., Jacob, D. J., Jimenez, J. L., Campuzano-Jost, P., Day, D. A., Hu, W., Krechmer,
783 J., Zhu, L., Kim, P. S., Miller, C. C., Fisher, J. A., Travis, K., Yu, K., Hanisco, T. F., Wolfe, G.
784 M., Arkinson, H. L., Pye, H. O. T., Froyd, K. D., Liao, J. and McNeill, V. F.: Aqueous-phase
785 mechanism for secondary organic aerosol formation from isoprene: Application to the Southeast
786 United States and co-benefit of SO2 emission controls, Atmos. Chem. Phys., 16, 1603–1618,

787 doi:10.5194/acp-16-1603-2016, 2016.
788 Marais, E. A., Jacob, D. J., Turner, J. R. and Mickley, L. J.: Evidence of 1991–2013 decrease of
789 biogenic secondary organic aerosol in response to SO2 emission controls, Environ. Sci.
790 Technol., 12, doi:https://doi.org/10.1088/1748-9326/aa69c8, 2017.
791 McNeill, V. F., Woo, J. L., Kim, D. D., Schwier, A. N., Wannell, N. J., Sumner, A. J. and
792 Barakat, J. M.: Aqueous-phase secondary organic aerosol and organosulfate formation in
793 atmospheric aerosols: A modeling study, Environ. Sci. Technol., 46(15), 8075–8081,
794 doi:10.1021/es3002986, 2012.
795 Murphy, D. M., Cziczo, D. J., Froyd, K. D., Hudson, P. K., Matthew, B. M., Middlebrook, A.
796 M., Peltier, R. E., Sullivan, A., Thomson, D. S. and Weber, R. J.: Single-peptide mass
797 spectrometry of tropospheric aerosol particles, J. Geophys. Res. Atmos., 111(23), 1–15,
798 doi:10.1029/2006JD007340, 2006.
799 Ng, N. L., Brown, S. S., Archibald, A. T., Atlas, E., Cohen, R. C., Crowley, J. N., Day, D. A.,
800 Donahue, N. M., Fry, J. L., Fuchs, H., Griffin, R. J., Guzman, M. I., Herrmann, H., Hodzic, A.,
801 Iinuma, Y., Kiendler-Scharr, A., Lee, B. H., Luecken, D. J., Mao, J., McLaren, R., Mutzel, A.,
802 Osthoff, H. D., Ouyang, B., Picquet-Varrault, B., Platt, U., Pye, H. O. T., Rudich, Y., Schwantes,
803 R. H., Shiraiwa, M., Stutz, J., Thornton, J. A., Tilgner, A., Williams, B. J. and Zaveri, R. A.:
804 Nitrate radicals and biogenic volatile organic compounds: Oxidation, mechanisms, and organic
805 aerosol, Atmos. Chem. Phys., 17(3), 2103–2162, doi:10.5194/acp-17-2103-2017, 2017.
806 Nguyen, T. B., Coggon, M. M., Bates, K. H., Zhang, X., Schwantes, R. H., Schilling, K. A.,
807 Loza, C. L., Flagan, R. C., Wennberg, P. O. and Seinfeld, J. H.: Organic aerosol formation from
808 the reactive uptake of isoprene epoxydiols (IEPOX) onto non-acidified inorganic seeds, Atmos.
809 Chem. Phys., 14(7), 3497–3510, doi:10.5194/acp-14-3497-2014, 2014.
810 Pai, S., Heald, C., Pierce, J., Farina, S., Marais, E., Jimenez, J., Campuzano-Jost, P., Nault, B.,
811 Middlebrook, A., Coe, H., Shilling, J., Bahreini, R., Dingle, J. and Vu, K.: An evaluation of
812 global organic aerosol schemes using airborne observations, Atmos. Chem. Phys., (20), 2637–
813 2665, doi:10.5194/acp-2019-331, 2020.
814 Pankow, J. F.: An Absorption-Model of the Gas Aerosol Partitioning Involved in the Formation
815 of Secondary Organic Aerosol, Atmos. Environ., 28(2), 189–193,
816 doi:10.1016/j.atmosenv.2007.10.060, 1994.
817 Paulot, F., Crounse, J. D., Kjaergaard, H. G., Kürten, A., Clair, J. M. S., Seinfeld, J. H. and
818 Wennberg, P. O.: Unexpected Epoxide Formation in the Gas-Phase Photooxidation of Isoprene,
819 Science (80-.)., 325, 730–734, doi:10.1126/science.1174251, 2009.
820 Paulot, F., Jacob, D. J., Pinder, R. W., Bash, J. O., Travis, K. R. and Henze, D. K.: Ammonia
821 emissions in the United States, European Union, and China derived by high-resolution inversion
822 of ammonium wet deposition data: Interpretation with a new agricultural emissions inventory
823 (MASAGE_NH3), J. Geophys. Res. Atmos., 119, 4343–4364, doi:doi:10.1002/2013JD021130,
824 2014.
825 Presto, A. a., Huff Hartz, K. E. and Donahue, N. M.: Secondary organic aerosol production from
826 terpene ozonolysis. 2. Effect of NOx concentration, Environ. Sci. Technol., 39(18), 7046–7054,
827 doi:10.1021/es050400s, 2005.
828 Pye, H. O. T., Liao, H., Wu, S., Mickley, L. J., Jacob, D. J., Henze, D. J. and Seinfeld, J. H.:
829 Effect of changes in climate and emissions on future sulfate-nitrate-ammonium aerosol levels in
830 the United States, J. Geophys. Res. Atmos., 114(1), 1–18, doi:10.1029/2008JD010701, 2009.
831 Pye, H. O. T., Chan, a. W. H., Barkley, M. P. and Seinfeld, J. H.: Global modeling of organic
832 aerosol: The importance of reactive nitrogen (NOx and NO3), Atmos. Chem. Phys., 10, 11261–

11276, doi:10.5194/acp-10-11261-2010, 2010.
Pye, H. O. T., Pinder, R. W., Piletic, I. R., Xie, Y., Capps, S. L., Lin, Y. H., Surratt, J. D., Zhang, Z., Gold, A., Luecken, D. J., Hutzell, W. T., Jaoui, M., Offenberg, J. H., Kleindienst, T. E., Lewandowski, M. and Edney, E. O.: Epoxide pathways improve model predictions of isoprene markers and reveal key role of acidity in aerosol formation, Environ. Sci. Technol., 47(19), 11056–11064, doi:10.1021/es402106h, 2013.
Pye, H. O. T., Murphy, B. N., Xu, L., Ng, N. L., Carlton, A. G., Guo, H., Weber, R., Vasilakos, P., Wyat Appel, K., Hapsari Budisulistiorini, S., Surratt, J. D., Nenes, A., Hu, W., Jimenez, J. L., Isaacman-Vanwertz, G., Misztal, P. K. and Goldstein, A. H.: On the implications of aerosol liquid water and phase separation for organic aerosol mass, Atmos. Chem. Phys., 17(1), 343–369, doi:10.5194/acp-17-343-2017, 2017.
Pye, H. O. T., D'Ambro, E. L., Lee, B. H., Schobesberger, S., Takeuchi, M., Zhao, Y., Lopez-Hilfiker, F., Liu, J., Shilling, J. E., Xing, J., Mathur, R., Middlebrook, A. M., Liao, J., Welti, A., Graus, M., Warneke, C., de Gouw, J. A., Holloway, J. S., Ryerson, T. B., Pollack, I. B. and Thornton, J. A.: Anthropogenic enhancements to production of highly oxygenated molecules from autoxidation, Proc. Natl. Acad. Sci. U. S. A., 116(14), 6641–6646, doi:10.1073/pnas.1810774116, 2019.
Pye, H. O. T., Nenes, A., Alexander, B., Ault, A. P., Barth, M. C., Simon, L., Collett, J. L., Fahey, K. M., Hennigan, C. J., Herrmann, H., Kanakidou, M., Kelly, J. T., Ku, I., Mcneill, V. F., Riemer, N., Shi, G., Tilgner, A., Walker, J. T., Wang, T., Weber, R., Xing, J., Zaveri, R. A. and Zuend, A.: The Acidity of Atmospheric Particles and Clouds, Atmos. Chem. Phys, 20, 4809–4888, doi:https://doi.org/10.5194/acp-20-4809-2020, 2020.
Randerson, J. T., van der Werf, G. R., Giglio, L., Collatz, G. J. and Kasibhatla, P. S.: Global Fire Emissions Database, Version 4, (GFEDv4), ORNL DAAC, doi:10.3334/ORNLDAAC/1293, 2015.
Ridley, D. A., Heald, C. L., Ridley, K. J. and Kroll, J. H.: Causes and consequences of decreasing atmospheric organic aerosol in the United States, Proc. Natl. Acad. Sci. U. S. A., 115(2), 290–295, doi:10.1073/pnas.1700387115, 2018.
Riedel, T. P., Lin, Y. H., Budisulistiorini, S. H., Gaston, C. J., Thornton, J. A., Zhang, Z., Vizuete, W., Gold, A. and Surratt, J. D.: Heterogeneous reactions of isoprene-derived epoxides: Reaction probabilities and molar secondary organic aerosol yield estimates, Environ. Sci. Technol. Lett., 2(2), 38–42, doi:10.1021/ez500406f, 2015.
Riedel, T. P., Lin, Y. H., Zhang, Z., Chu, K., Thornton, J. A., Vizuete, W., Gold, A. and Surratt, J. D.: Constraining condensed-phase formation kinetics of secondary organic aerosol components from isoprene epoxydiols, Atmos. Chem. Phys., 16(3), 1245–1254, doi:10.5194/acp-16-1245-2016, 2016.
Riva, M., Bell, D. M., Hansen, A. M. K., Drozd, G. T., Zhang, Z., Gold, A., Imre, D., Surratt, J. D., Glasius, M. and Zelenyuk, A.: Effect of Organic Coatings, Humidity and Aerosol Acidity on Multiphase Chemistry of Isoprene Epoxydiols, Environ. Sci. Technol., 50(11), 5580–5588, doi:10.1021/acs.est.5b06050, 2016.
Riva, M., Chen, Y., Zhang, Y., Lei, Z., Olson, N. E., Boyer, H. C., Narayan, S., Yee, L. D., Green, H. S., Cui, T., Zhang, Z., Baumann, K., Fort, M., Edgerton, E., Budisulistiorini, S. H., Rose, C. A., Ribeiro, I. O., e Oliveira, R. L., dos Santos, E. O., Machado, C. M. D., Szopa, S., Zhao, Y., Alves, E. G., de Sá, S. S., Hu, W., Knipping, E. M., Shaw, S. L., Duvoisin Junior, S., de Souza, R. A. F., Palm, B. B., Jimenez, J.-L., Glasius, M., Goldstein, A. H., Pye, H. O. T., Gold, A., Turpin, B. J., Vizuete, W., Martin, S. T., Thornton, J. A., Dutcher, C. S., Ault, A. P.

879 and Surratt, J. D.: Increasing Isoprene Epoxydiol-to-Inorganic Sulfate Aerosol Ratio Results in
880 Extensive Conversion of Inorganic Sulfate to Organosulfur Forms: Implications for Aerosol
881 Physicochemical Properties, Environ. Sci. Technol., 53(15), 8682–8694,
882 doi:10.1021/acs.est.9b01019, 2019.
883 Schmedding, R., Ma, M., Zhang, Y., Farrell, S., Pye, H. O. T., Chen, Y., Wang, C. tsan, Rasool,
884 Q. Z., Budisulistiorini, S. H., Ault, A. P., Surratt, J. D. and Vizuete, W.: A-Pinene-Derived
885 organic coatings on acidic sulfate aerosol impacts secondary organic aerosol formation from
886 isoprene in a box model, Atmos. Environ., 213(June), 456–462,
887 doi:10.1016/j.atmosenv.2019.06.005, 2019.
888 Schroder, J. C., Campuzano-Jost, P., Day, D. A., Shah, V., Larson, K., Sommers, J. M., Sullivan,
889 A. P., Campos, T., Reeves, J. M., Hills, A., Hornbrook, R. S., Blake, N. J., Scheuer, E., Guo, H.,
890 Fibiger, D. L., McDuffie, E. E., Hayes, P. L., Weber, R. J., Dibb, J. E., Apel, E. C., Jaeglé, L.,
891 Brown, S. S., Thornton, J. A. and Jimenez, J. L.: Sources and Secondary Production of Organic
892 Aerosols in the Northeastern United States during WINTER, J. Geophys. Res. Atmos., 123(14),
893 7771–7796, doi:10.1029/2018JD028475, 2018.
894 Schwantes, R. H., Charan, S. M., Bates, K. H., Huang, Y., Nguyen, T. B., Mai, H., Kong, W.,
895 Flagan, R. C. and Seinfeld, J. H.: Low-volatility compounds contribute significantly to isoprene
896 secondary organic aerosol (SOA) under high-NOx conditions, Atmos. Chem. Phys., 19(11),
897 7255–7278, doi:10.5194/acp-19-7255-2019, 2019.
898 Shah, V., Jaeglé, L., Jimenez, J. L., Schroder, J. C., Campuzano-Jost, P., Campos, T. L., Reeves,
899 J. M., Stell, M., Brown, S. S., Lee, B. H., Lopez-Hilfiker, F. D. and Thornton, J. A.: Widespread
900 Pollution From Secondary Sources of Organic Aerosols During Winter in the Northeastern
901 United States, Geophys. Res. Lett., 46(5), 2974–2983, doi:10.1029/2018GL081530, 2019.
902 Shephard, M. W. and Cady-Pereira, K. E.: Cross-track Infrared Sounder (CrIS) satellite
903 observations of tropospheric ammonia, Atmos. Meas. Tech., 8(3), 1323–1336, doi:10.5194/amt-
904 8-1323-2015, 2015.
905 Shrivastava, M., Cappa, C. D., Fan, J., Goldstein, A. H., Guenther, A. B., Jimenez, J. L., Kuang,
906 C., Laskin, A., Martin, S. T., Ng, N. L., Petaja, T., Pierce, J. R., Rasch, P. J., Roldin, P., Seinfeld,
907 J. H., Shilling, J., Smith, J. N., Thornton, J. A., Volkamer, R., Wang, J., Worsnop, D. R., Zaveri,
908 R. A., Zelenyuk, A. and Zhang, Q.: Recent advances in understanding secondary organic aerosol:
909 Implications for global climate forcing, Rev. Geophys., 55(2), 509–559,
910 doi:10.1002/2016RG000540, 2017.
911 Shrivastava, M., Andreae, M. O., Artaxo, P., Barbosa, H. M. J., Berg, L. K., Brito, J., Ching, J.,
912 Easter, R. C., Fan, J., Fast, J. D., Feng, Z., Fuentes, J. D., Glasius, M., Goldstein, A. H., Alves, E.
913 G., Gomes, H., Gu, D., Guenther, A., Jathar, S. H., Kim, S., Liu, Y., Lou, S., Martin, S. T.,
914 McNeill, V. F., Medeiros, A., de Sá, S. S., Shilling, J. E., Springston, S. R., Souza, R. A. F.,
915 Thornton, J. A., Isaacman-VanWertz, G., Yee, L. D., Ynoue, R., Zaveri, R. A., Zelenyuk, A. and
916 Zhao, C.: Urban pollution greatly enhances formation of natural aerosols over the Amazon
917 rainforest, Nat. Commun., 10(1), doi:10.1038/s41467-019-08909-4, 2019.
918 Silvern, R. F., Jacob, D. J., Kim, P. S., Marais, E. A., Turner, J. R., Campuzano-Jost, P. and
919 Jimenez, J. L.: Inconsistency of ammonium-sulfate aerosol ratios with thermodynamic models in
920 the eastern US: A possible role of organic aerosol, Atmos. Chem. Phys., 17(8), 5107–5118,
921 doi:10.5194/acp-17-5107-2017, 2017.
922 Solomon, P. A., Crumpler, D., Flanagan, J. B., Jayanty, R. K. M., Rickman, E. E. and McDade,
923 C. E.: U.S. National PM2.5 chemical speciation monitoring networks—CSN and IMPROVE:
924 Description of networks, J. Air Waste Manag. Assoc., 64(12), 1410–1438,

925 doi:10.1080/10962247.2014.956904, 2014.
926 Song, S., Gao, M., Xu, W., Shao, J., Shi, G., Wang, S., Wang, Y., Sun, Y. and McElroy, M. B.:
927 Fine-particle pH for Beijing winter haze as inferred from different thermodynamic equilibrium
928 models, Atmos. Chem. Phys., 18(10), 7423–7438, doi:10.5194/acp-18-7423-2018, 2018.
929 Surratt, J. D., Lewandowski, M., Offenberg, J. H., Jaoui, M., Kleindienst, T. E., Edney, E. O. and
930 Seinfeld, J. H.: Effect of acidity on secondary organic aerosol formation from isoprene, Environ.
931 Sci. Technol., (41), 5363–5369, doi:10.1021/es0704176, 2007a.
932 Surratt, J. D., Kroll, J. H., Kleindienst, T. E., Edney, E. O., Claeys, M., Sorooshian, A., Ng, N.
933 L., Offenberg, J. H., Lewandowski, M., Jaoui, M., Flagan, R. C. and Seinfeld, J. H.: Evidence for
934 organosulfates in secondary organic aerosol, Environ. Sci. Technol., (41), 517–527,
935 doi:10.1021/es062081q, 2007b.
936 Surratt, J. D., Chan, A. W. H., Eddingsaas, N. C., Chan, M., Loza, C. L., Kwan, A. J., Hersey, S.
937 P., Flagan, R. C., Wennberg, P. O. and Seinfeld, J. H.: Reactive intermediates revealed in
938 secondary organic aerosol formation from isoprene, Proc. Natl. Acad. Sci., 107(15), 6640–6645,
939 doi:10.1073/pnas.0911114107, 2010.
940 Tan, Y., Lim, Y. B., Altieri, K. E., Seitzinger, S. P. and Turpin, B. J.: Mechanisms leading to
941 oligomers and SOA through aqueous photooxidation: Insights from OH radical oxidation of
942 acetic acid and methylglyoxal, Atmos. Chem. Phys., 12(2), 801–813, doi:10.5194/acp-12-801-
943 2012, 2012.
944 Tao, Y. and Murphy, J. G.: The sensitivity of PM2.5 acidity to meteorological parameters and
945 chemical composition changes: 10-year records from six Canadian monitoring sites, Atmos.
946 Chem. Phys. Discuss., 1–21, doi:10.5194/acp-2019-238, 2019.
947 Travis, K. R., Jacob, D. J., Fisher, J. A., Kim, P. S., Marais, E. A., Zhu, L., Yu, K., Miller, C. C.,
948 Yantosca, R. M., Sulprizio, M. P., Thompson, A. M., Wennberg, P. O., Crounse, J. D., St Clair,
949 J. M., Cohen, R. C., Laughner, J. L., Dibb, J. E., Hall, S. R., Ullmann, K., Wolfe, G. M., Pollack,
950 I. B., Peischl, J., Neuman, J. A. and Zhou, X.: Why do models overestimate surface ozone in the
951 Southeast United States?, Atmos. Chem. Phys., 16(21), 13561–13577, doi:10.5194/acp-16-
952 13561-2016, 2016.
953 Tsui, W. G., Woo, J. L. and Mcneill, V. F.: Impact of Aerosol-Cloud Cycling on Aqueous
954 Secondary Organic Aerosol Formation, Atmosphere (Basel)., 10, 666,
955 doi:doi:10.3390/atmos10110666, 2019.
956 Wagner, N. L., Brock, C. A., Angevine, W. M., Beyersdorf, A., Campuzano-Jost, P., Day, D., De
957 Gouw, J. A., Diskin, G. S., Gordon, T. D., Graus, M. G., Holloway, J. S., Huey, G., Jimenez, J.
958 L., Lack, D. A., Liao, J., Liu, X., Markovic, M. Z., Middlebrook, A. M., Mikoviny, T., Peischl,
959 J., Perring, A. E., Richardson, M. S., Ryerson, T. B., Schwarz, J. P., Warneke, C., Welti, A.,
960 Wisthaler, A., Ziemba, L. D. and Murphy, D. M.: In situ vertical profiles of aerosol extinction,
961 mass, and composition over the southeast United States during SENEX and SEAC4RS:
962 Observations of a modest aerosol enhancement aloft, Atmos. Chem. Phys., 15(12), 7085–7102,
963 doi:10.5194/acp-15-7085-2015, 2015.
964 Weber, R. J., Guo, H., Russell, A. G. and Nenes, A.: High aerosol acidity despite declining
965 atmospheric sulfate concentrations over the past 15 years, Nat. Geosci., 9,
966 doi:10.1038/NGEO2665, 2016.
967 Woo, J. L. and McNeill, V. F.: simpleGAMMA v1.0 - A reduced model of secondary organic
968 aerosol formation in the aqueous aerosol phase (aaSOA), Geosci. Model Dev., 8(6), 1821–1829,
969 doi:10.5194/gmd-8-1821-2015, 2015.
970 Worton, D. R., Surratt, J. D., Lafranchi, B. W., Chan, A. W. H., Zhao, Y., Weber, R. J., Park, J.

H., Gilman, J. B., De Gouw, J., Park, C., Schade, G., Beaver, M., Clair, J. M. S., Crounse, J., Wennberg, P., Wolfe, G. M., Harrold, S., Thornton, J. A., Farmer, D. K., Docherty, K. S., Cubison, M. J., Jimenez, J. L., Frossard, A. A., Russell, L. M., Kristensen, K., Glasius, M., Mao, J., Ren, X., Brune, W., Browne, E. C., Pusede, S. E., Cohen, R. C., Seinfeld, J. H. and Goldstein, A. H.: Observational insights into aerosol formation from isoprene, Environ. Sci. Technol., (47), 11403–11413, doi:10.1021/es4011064, 2013.

Xu, L., Suresh, S., Guo, H., Weber, R. J. and Ng, N. L.: Aerosol characterization over the southeastern United States using high-resolution aerosol mass spectrometry: Spatial and seasonal variation of aerosol composition and sources with a focus on organic nitrates, Atmos. Chem. Phys., 15(13), 7307–7336, doi:10.5194/acp-15-7307-2015, 2015a.

Xu, L., Guo, H., Boyd, C. M., Klein, M., Bougiatioti, A., Cerully, K. M., Hite, J. R., Isaacman-VanWertz, G., Kreisberg, N. M., Knote, C., Olson, K., Koss, A., Goldstein, A. H., Hering, S. V., de Gouw, J., Baumann, K., Lee, S.-H., Nenes, A., Weber, R. J. and Ng, N. L.: Effects of anthropogenic emissions on aerosol formation from isoprene and monoterpenes in the southeastern United States, Proc. Natl. Acad. Sci., 112(1), 37–42, doi:10.1073/pnas.1417609112, 2015b.

Xu, L., Middlebrook, A. M., Liao, J., de Gouw, J. A., Guo, H., Weber, R. J., Nenes, A., Lopez-Hilfiker, F. D., Lee, B. H., Thornton, J. A., Brock, C. A., Neuman, J. A., Nowak, J. B., Pollack, I. B., Welti, A., Graus, M., Warneke, C. and Ng, N. L.: Enhanced formation of isoprene-derived organic aerosol in sulfur-rich power plant plumes during Southeast Nexus, J. Geophys. Res., 121, 11137–11153, doi:10.1002/2016JD025156, 2016.

Xu, L., Pye, H. O. T., He, J., Chen, Y., Murphy, B. N. and Ng, N. L.: Experimental and model estimates of the contributions from biogenic monoterpenes and sesquiterpenes to secondary organic aerosol in the southeastern United States, Atmos. Chem. Phys., 18(17), 12613–12637, doi:10.5194/acp-18-12613-2018, 2018.

Yu, K., Jacob, D. J., Fisher, J. A., Kim, P. S., Marais, E. A., Miller, C. C., Travis, K. R., Zhu, L., Yantosca, R. M., Sulprizio, M. P., Cohen, R. C., Dibb, J. E., Fried, A., Mikoviny, T., Ryerson, T. B., Wennberg, P. O. and Wisthaler, A.: Sensitivity to grid resolution in the ability of a chemical transport model to simulate observed oxidant chemistry under high-isoprene conditions, Atmos. Chem. Phys., 16(7), 4369–4378, doi:10.5194/acp-16-4369-2016, 2016.

Zhang, H., Yee, L. D., Lee, B. H., Curtis, M. P., Worton, D. R., Isaacman-VanWertz, G., Offenberg, J. H., Lewandowski, M., Kleindienst, T. E., Beaver, M. R., Holder, A. L., Lonneman, W. A., Docherty, K. S., Jaoui, M., Pye, H. O. T., Hu, W., Day, D. A., Campuzano-Jost, P., Jimenez, J. L., Guo, H., Weber, R. J., de Gouw, J., Koss, A. R., Edgerton, E. S., Brune, W., Mohr, C., Lopez-Hilfiker, F. D., Lutz, A., Kreisberg, N. M., Spielman, S. R., Hering, S. V., Wilson, K. R., Thornton, J. A. and Goldstein, A. H.: Monoterpenes are the largest source of summertime organic aerosol in the southeastern United States, Proc. Natl. Acad. Sci., 201717513, doi:10.1073/pnas.1717513115, 2018a.

Zhang, Y., Chen, Y., Lambe, A. T., Olson, N. E., Lei, Z., Craig, R. L., Zhang, Z., Gold, A., Onasch, T. B., Jayne, J. T., Worsnop, D. R., Gaston, C. J., Thornton, J. A., Vizuete, W., Ault, A. P. and Surratt, J. D.: Effect of the Aerosol-Phase State on Secondary Organic Aerosol Formation from the Reactive Uptake of Isoprene-Derived Epoxydiols (IEPOX), Environ. Sci. Technol. Lett., 5(3), 167–174, doi:10.1021/acs.estlett.8b00044, 2018b.

Zhang, Y., Chen, Y., Lei, Z., Olson, N. E., Riva, M., Koss, A. R., Zhang, Z., Gold, A., Jayne, J. T., Worsnop, D. R., Onasch, T. B., Kroll, J. H., Turpin, B. J., Ault, A. P. and Surratt, J. D.: Joint Impacts of Acidity and Viscosity on the Formation of Secondary Organic Aerosol from Isoprene

Epoxydiols (IEPOX) in Phase Separated Particles, ACS Earth Sp. Chem., 3(12), 2646–2658, doi:10.1021/acsearthspacechem.9b00209, 2019a.
Zhang, Y., Nichman, L., Spencer, P., Jung, J. I., Lee, A., Heffernan, B. K., Gold, A., Zhang, Z., Chen, Y., Canagaratna, M. R., Jayne, J. T., Worsnop, D. R., Onasch, T. B., Surratt, J. D., Chandler, D., Davidovits, P. and Kolb, C. E.: The Cooling Rate- And Volatility-Dependent Glass-Forming Properties of Organic Aerosols Measured by Broadband Dielectric Spectroscopy, Environ. Sci. Technol., 53(21), 12366–12378, doi:10.1021/acs.est.9b03317, 2019b.
Zheng, Y., Unger, N., Hodzic, A., Emmons, L., Knote, C., Tilmes, S., Lamarque, J. F. and Yu, P.: Limited effect of anthropogenic nitrogen oxides on secondary organic aerosol formation, Atmos. Chem. Phys., 15(23), 13487–13506, doi:10.5194/acp-15-13487-2015, 2015.
Ziemann, P. J. and Atkinson, R.: Kinetics, products, and mechanisms of secondary organic aerosol formation, Chem. Soc. Rev., 41(19), 6582, doi:10.1039/c2cs35122f, 2012.

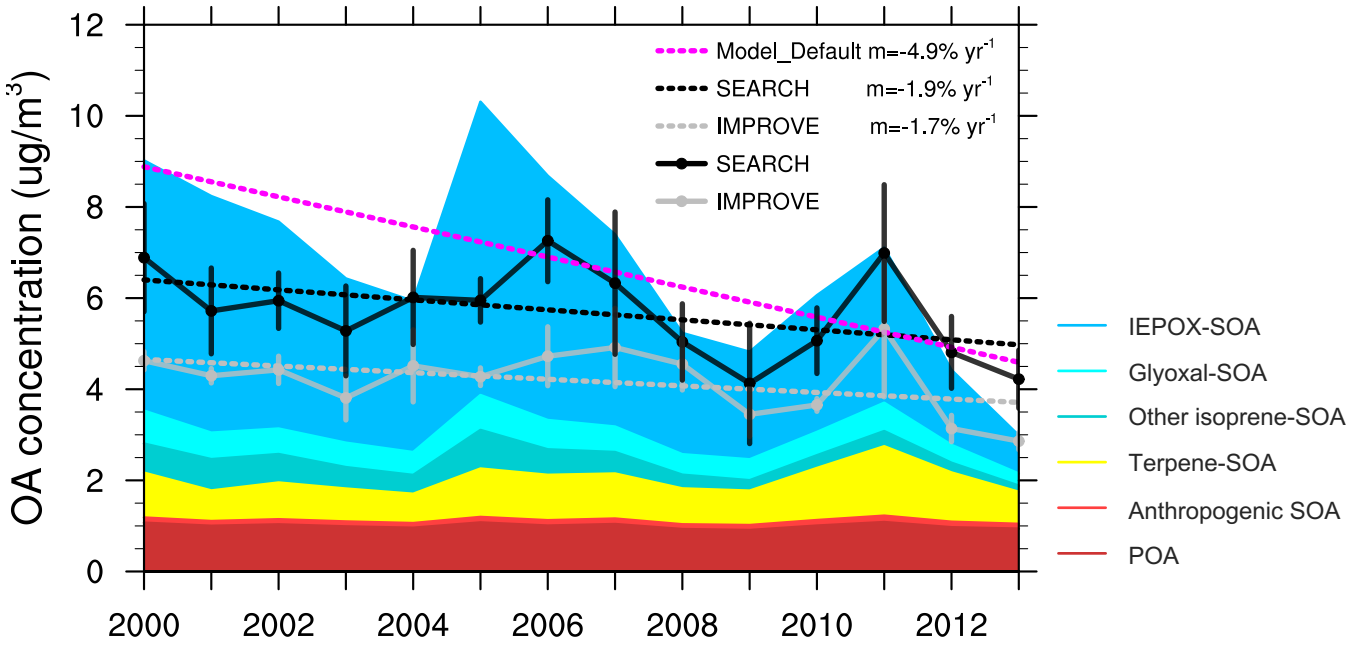

Figure 1. Comparison of June-July-August averaged surface OA concentration (μg/m^3) over the southeast US between the default model and the observation from IMPROVE and SEARCH network. Colored shades represent different components of modeled OA. IEPOX-, glyoxal-, and other isoprene-SOA are from aqueous uptake of isoprene oxidation products. Terpene- and anthropogenic SOA are dry SOA calculated using volatility-basis-set.

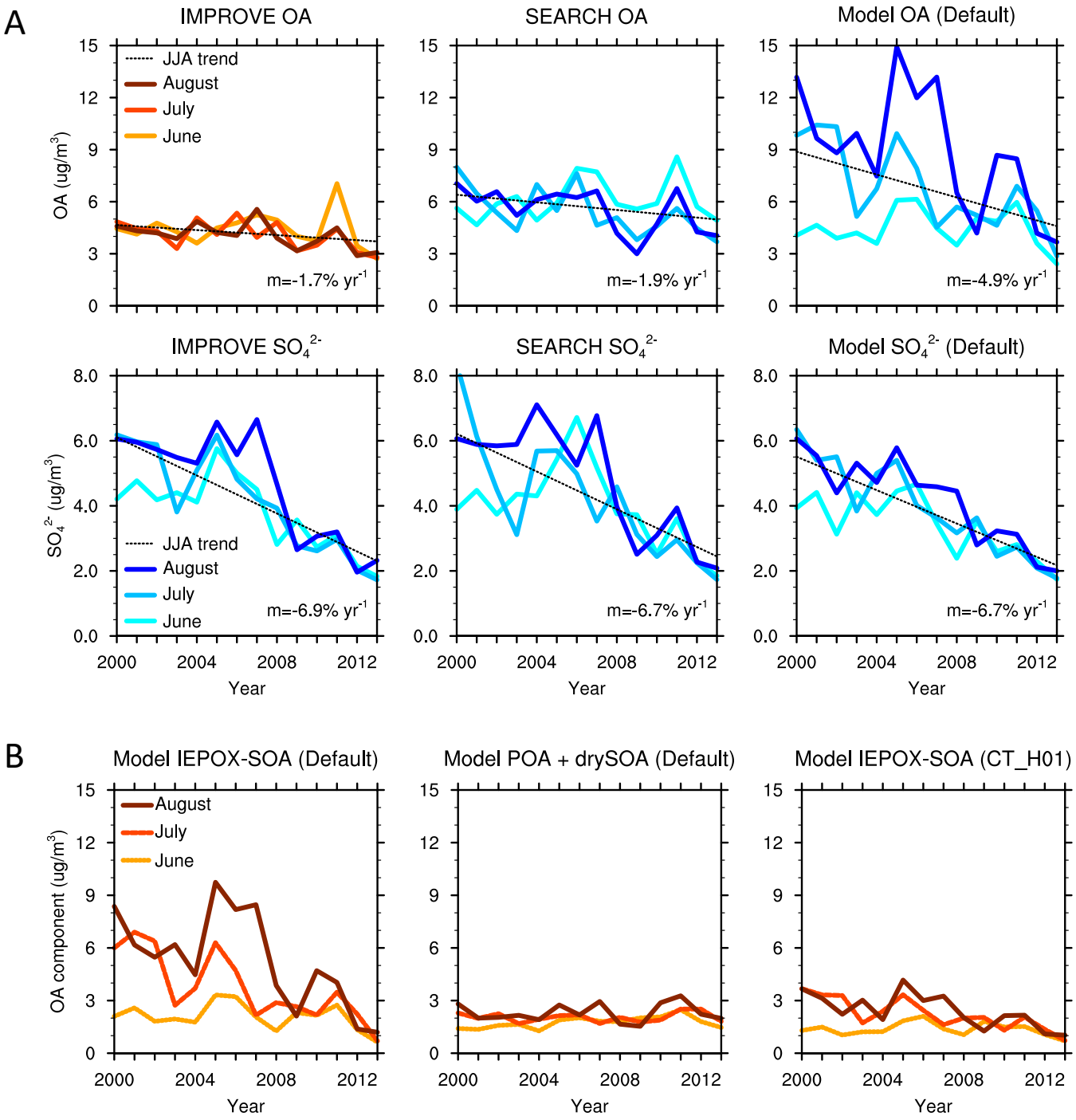

Figure 2. (A) Monthly surface OA and sulfate (SO_4^{2-}) concentration (μg/m^3) averaged over the southeast US from IMPROVE, SEARCH and the default model. **(B)** Monthly surface concentrations of IEPOX-SOA and the sum of POA and dry SOA from the default model, and IEPOX-SOA from the CT_H01 simulation.

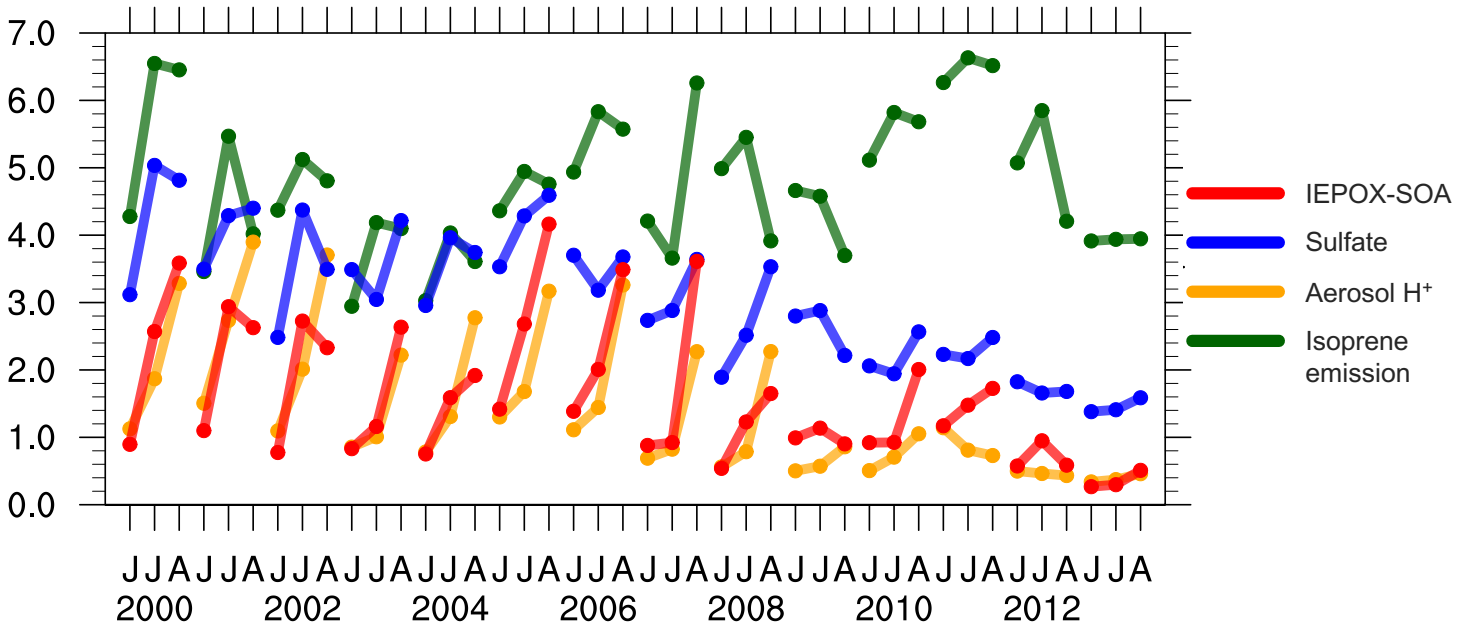

Figure 3. Standardized monthly surface IEPOX-SOA concentration, sulfate concentration, aerosol H^+ activity and isoprene emission from the default model. All variables are averaged over the southeast US, and have been divided by 1 standard deviations, therefore are unitless.

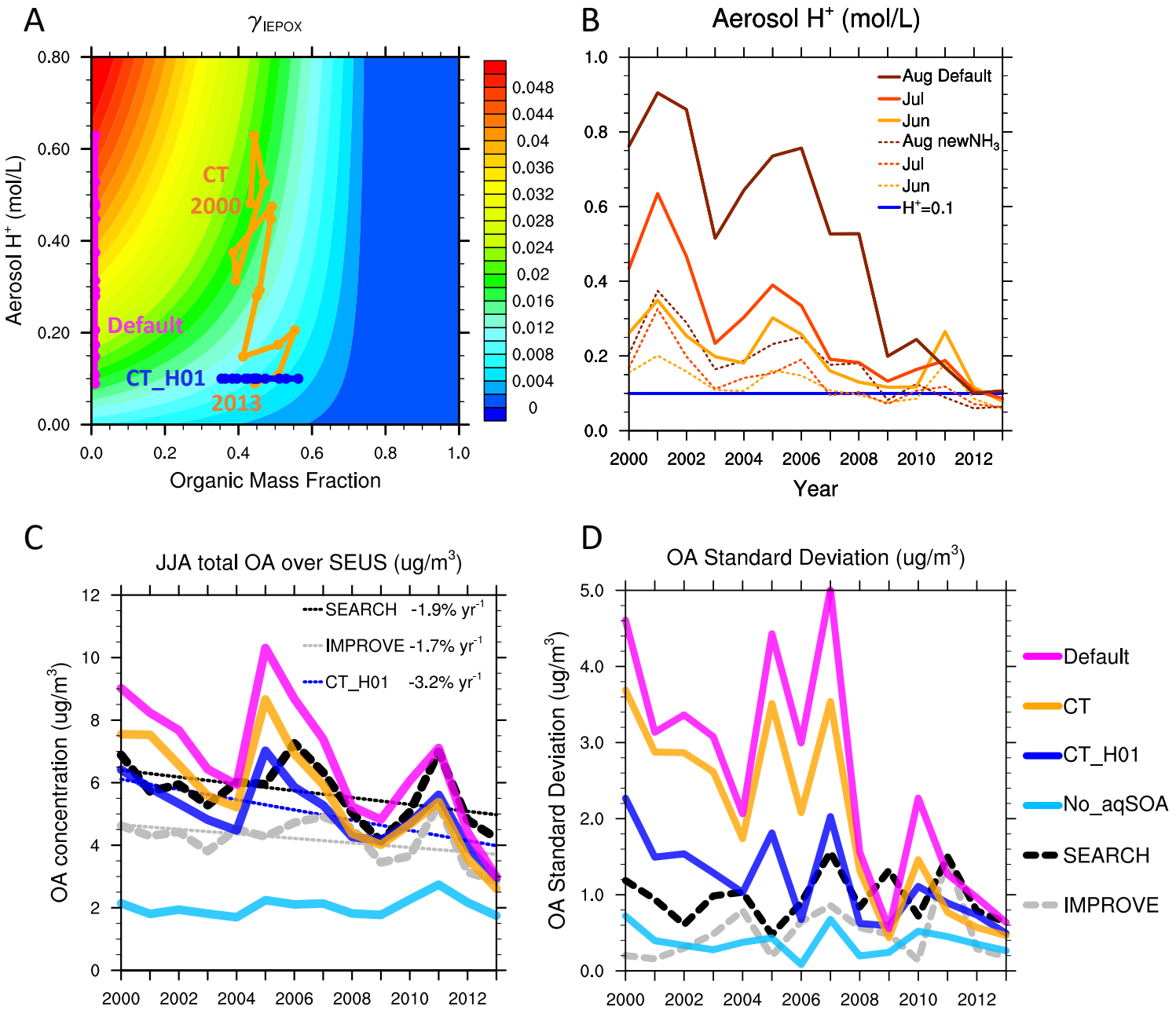

Figure 4. **(A)** Schematic diagram of IEPOX reactive uptake coefficient (γ_{IEPOX}). Colored lines indicate the position of JJA-averaged organic mass fraction and aerosol H^+ activity in 2000-2013 from the 'Default', 'CT' and 'CT_H01' simulations. **(B)** Simulated aerosol acidity (mol/L) from the default, 'CT_newNH$_3$' and 'CT_H01' simulations. **(C)** JJA-averaged surface OA (μg/m^3) from IMPROVE, SEARCH and all model simulations. **(D)** Standard deviation of OA (μg/m^3) between June, July and August from IMPROVE, SEARCH and all model simulations. All results are averaged over the southeast US.

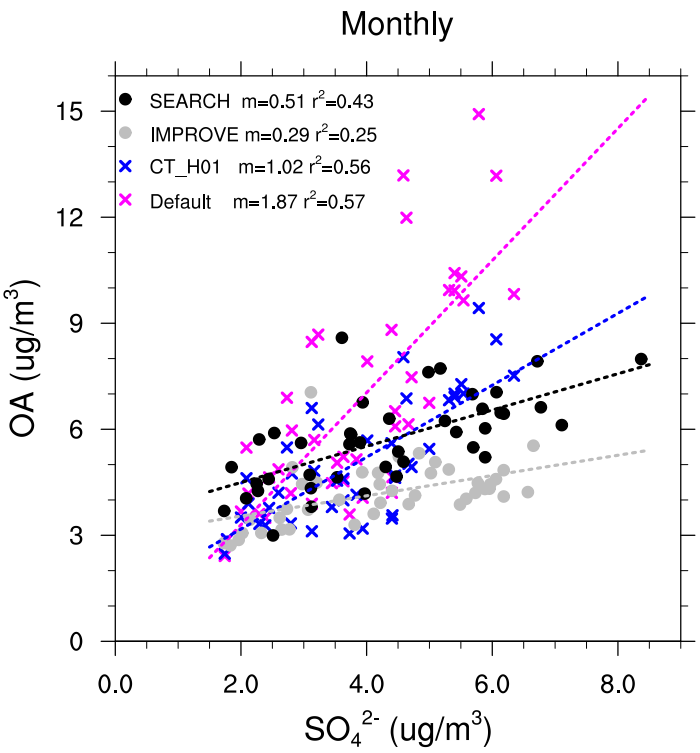

Figure 5. Relationships between monthly OA and sulfate concentrations (μg/m^3). Each dot represents monthly data averaged from all sites from each network within the southeast US.